POUSSIX CEA/DEBENE
Irradiation Experiment in PHENIX

O. Götzmann
Institut für Materialforschung
Projekt Nukleare Sicherheitsforschung

Kernforschungszentrum Karlsruhe

KfK 5419

POUSSIX
CEA/DEBENE
Irradiation Experiment in PHENIX

O. Götzmann

Abstract

POUSSIX was a common irradiation experiment in the frame of the CEA/DEBENE fast breeder co-operation to test the behaviour of high density fuel at high burn-up. Twelve pins of German (8) and Belgian (4) fabrication were irradiated in the French fast breeder reactor PHENIX. The irradiation lasted from October 1984 until July 1987. Part of the non-destrucive PIE was performed in Cadarache, whilst three pins were destructively examined in Karlsruhe. The primary test parameter was the smear density; it ranged from 88 to 92 % TD. The fuel-to-cladding gap size served as a secondary parameter with diametral values of 100 to 275 µm.

All pins performed well. Fuel cladding mechanical interactions remained small, even after a burn-up of almost 10 at %. The cladding expansions can essentially be blamed on the effects of the fast flux on the cladding steel 1.4970 cw, a. At a dose of 113 dpa F (85dpa NRT), the maximum diametral increase was 65 µm or 0.9 %. High smear density had no adverse effects on pin behaviour. Pins with small gaps behaved rather better than those with large gaps. The central hole in the annular pellet pins did not remain hollow over the entire length of the fuel column. There were blockages at both ends due to fuel condensation, and also towards the pin mid-section due to metallic fission product ingots.

Re-irradiation of two of the pins in HFR Petten, with a power transient of over 150 %, appeared to do no harm to the pins.

POUSSIX CEA/DEBENE Bestrahlungsexperiment im PHENIX

Zusammenfassung

POUSSIX war ein gemeinsames Bestrahlungsexperiment im Rahmen der Schnellbrüterzusammenarbeit von CEA und DEBENE zur Untersuchung des Verhaltens von hochdichtem Brennstoff bei hohen Abbränden. Insgesamt zwölf Stäbe aus deutscher (8) und belgischer (4) Fertigung wurden im französischen Schnellen Brutreaktor PHENIX bestrahlt. Die Bestrahlung dauerte von Oktober 1984 bis Juli 1987. Ein Teil der nicht-zerstörenden Nachuntersuchung wurde in Cadarache, die zerstörende Nachuntersuchung an 3 Stäben in Karlsruhe durchgeführt. Der primäre Versuchsparameter war die Schmierdichte, sie betrug zwischen 88 und 92 % TD. Als sekundärer Versuchsparameter diente die Brennstoff/Hülle Spaltgröße, sie reichte von 100 bis 275 µm diametral.

Alle Stäbe verhielten sich gut. Die mechanischen Wechselwirkungen blieben auch nach einem Abbrand von fast 10 at % gering. Für die Hüllaufweitungen muß in erster Linie die Wirkung des schnellen Flusses auf den Hüllstahl (1.4970 cw,a) verantwortlich gemacht werden. Bei einer Dosis von 113 dpa F (85 dpa NRT) betrug die maximale Druchmesservergrößerung 65 µm oder 0.9 %. Die hohe Schmierdichte hatte keine nachteiligen Auswirkungen auf das Stabverhalten. Die Stäbe mit kleinerem Spalt verhielten sich eher besser als die mit großem Spalt. Der zentrale Hohlraum in den Ringtablettensäulen blieb nicht hohl über die gesamte Säulenlänge. An beiden Enden gab es Verstopfungen durch Brennstoffkondensation, und weiter in Stabmitte auch solche durch Ausscheidungen (ingots) metallischer Spaltprodukte.

Eine Nachbestrahlung im HFR Petten mit einer Leistungstransienten von über 150 % haben die zwei dabei eingesetzten hochabgebrannten Stäbe gut überstanden.

Contents

1.   Introduction

The POUSSIX irradiation was planned as a common experiment in the frame of the CEA/DEBENE fast breeder co-operation to evaluate the performance of high density fuel pins at high burn-up. Fuel pins were fabricated by ALKEM/Germany, and by Belgonucleaire and CEN/MOL, Belgium. The irradiation took place in the reactor PHENIX, France. Planning of the test started in 1979, irradiation started in October 1984 and lasted until July 1987, non-destructive testing was performed in 1988, and destructive testing on a few pins in 1993.

The aim of the experiment was to optimize fuel smear density and the size of the gap between fuel and cladding with respect to mechanical interactions between fuel and cladding (FCMI) at medium and high burn-up. Pins of Mk II type for the SNR 300 should be used with high bulk density fuel of good solubility. A comparison of dispersion hardened ferritic claddings with standard ones of 1.4970 cw steel should be possible.

The responsibility for fabrication lay with the German and Belgian teams, the French took care of the irradiation. The first non-destructive testing was performed in the LDAC in Cadarache. The destructive PIE work described in this report was supplied by the Hot Cells at KfK.

2.   Experimental

2.1   Fuel pin fabrication

The fuel pin was of Mk II type, that means, a pin diameter of 7,6 mm, a mixed uranium-plutonium oxide fuel with natural or depleted uranium, a plutonium content around 20 %, a bulk density of 92 % TD, and a cladding of 1.4970 cw steel. All fuel and pin characteristics of the pins employed in the test /1/ are given in table 1. Some confusion about pin numbers may arise in looking at the various reports on fabrication and results. In French reports, the order numbers are used as the pin numbers. In German and Belgian reports, the pin markings, either in full or just the pertaining figures, are referred to as pin numbers. In this report the pin numbers consist of two figures separated by a slash: the first figure will be the order number (French), and the second figure is taken from the markings (DEBENE). For example, the pin with the marking POU 01 and the order number 7 will be referred to as pin 7/1. Likewise, pin 2/11 means the pin with the French number (order number) 2 and DEBENE number (marking)11.

Table 1: Fuel and Pin Characteristics

Fabrication	German (ALKEM)								Belgian (Belgonucl.)			
Cladding	1.4970 15 % cw, a										DT2203Yo5	
Order No.	1	2	3	4	5	6	7	8	9	10	11	12
Markings	Pou 08	Pou 11	Pou 18	Pou 19	Pou 04	Pou 14	Pou 01	Pou 02	Po21	Po 23	Po 30	Po 32
Pellet dia [mm]	6.325	6.325	6.415	6.415	6.474	6.483	6.417	6.417	6.504	6.504	6.416	6.416
P. inner hole. [mm]	-	-	-	-	-	-	1.233	1.233	-	-	-	-
Gap diam. [μm]	273	277	183	184	127	117	182	181	96	96	96	174
Bulk dens. % TD	96	96	97.7	97.7	96	96	96.5	96.5	94.6	94.6	95.7	95.7
Smear dens. % TD	88	88	92.4	92.4	92.6	92.6	88	88	91.9	91.9	90.7	90.7
Col. length [mm]	748.3	747.4	753.5	747.0	753.5	747.4	750.2	748.3	750.3	749.5	752.7	747
O/M-ratio	1.955	1.955	1.954	1.954	1.955	1.958	1.957	1.957	1.964	1.964	1.964	1.964
Pu/U+Pu	21.2	21.2	21.9	21.9	21.2	21.2	21.2	21.2	21	21	21	21
Pu_f/Pu	75.78	75.78	71.02	71.02	75.86	75.86	75.78	75.78	78.39	78.39	78.39	78.39

Pin length [mm]   1500 ±2
Pin outer diam [mm]   7.6 ±0.03
Clad inner diam [mm]   6.6 ±0.03
Wall thickness [mm]   0.5

The primary test parameter was the smear density with values of 88; 90 and 92 % TD, with emphasis on 88 and 92 % TD. The secondary parameter was the variation in the initial void volume distribution. Void volume other than porosity could be accommodated in a large gap or in an inner hole. With these parameter variations we obtained six pin varieties. For each variety two pins were employed.

2.2   Irradiation

The twelve wire-spaced pins were assembled in a DIMEP capsule and irradiated in the PHENIX reactor from 13th of October 1984 until 15th July 1987. Following 587 equivalent full power days, the fuel reached a maximum burn-up of 9,57 at % and the cladding a dose of 113 dpa F (or 85 dpa NRT). The experiment started in the 5th row (couronne) of the reactor core with an intermediate power level of around 325 W/cm maximum for about 30 days to undergo the so-called "vaccination". Later it was moved to the 4th row in order to attain its full power. Near full power, however, was attained only during a short period of some 10 days before the reactor power was reduced to 2/3 of its nominal load. Only after 3 reactor cycles in operation or 200 equivalent full power days did the maximum linear power come close to 450 W/cm. Prior to this, the maximum power level was, except for that intermittent 10 days period, below 350 W/cm. The irradiation history in terms of linear power and nominal (mid wall) cladding temperature for the highest charged pin 5/4 is given in figs. 1 and 2. The difference in linear power between the pins is directly coupled with their filling (or smear-) density. The highest values for power and nominal cladding temperature during the irradiation for each pin are given in table 2.

3.   Results

3.1   Non-destructive testing

3.1.1   Pin measurements

The results of the measurements on the outside of the pins in terms of diameter and length changes are listed in table 4. The axial diametral profiles for each pair of the same pin type are shown in fig. 3. Only two of the Belgian pins had their profiles taken. On their sister pins, the spacers were kept in place for re-irradiation. As fig. 3 indicates, the maximum increase occurred, in general, on the lower fuel end. Exceptions are the ferritic pin with very little diametral change and the pin with the smallest gap where the diametral expansion is almost uniform over 3/4 of the pin's length. There is little diametral change in the upper 150 mm of the fuel column for each pin.

- 4 -

Table 2: Maximum power and cladding temperature values for each pin

PIN	Linear power W/cm	Nominal cladding temperature °C
1/8	420	620
2/11	418	619
3/18	440	630
4/19	436	627
5/4	447	635
6/14	441	631
7/1	421	620
8/2	420	620
9/21	440	630
10/23	440	630
11/30	432	626
12/32	429	624

Table 3: Fission gas release and free volume

PIN		2/11	7/1	5/4
free volume PIE	cm³	25	24,6	24,2
free volume initial	cm³	23,4	23,5	22
free vol. change	%	6,5	4	9
fuel mass	g	245	246	259
mean b. u.	at %	8,16	8,16	8,16
Kr released	cm³	-	-	27,663
Xe released	cm³	-	-	258,525
Kr-85 released	GBq	85,5	81	86
Xe/Kr-ratio		-	-	9,35
fission gas generated	cm³	414	415	437
fission gas released	cm³	284,5*	269,5*	286,2
fission gas release ratio	%	68,7	64,9	65,5

* determined from Kr-85 activity

Table 4: Results obtained from non-destructive examination*

Pin	Initial f-cl. gap μm	Diam. change pin μm	Ovalisation pin μm	Length change		Effect. Temp. °C	Central hole length		Fuel bridge on ends	
				pin mm	f - column mm		neutron. mm	Betatr. mm	lower mm	upper mm
1/8	273	54	32	3.3	20	2500	456			
2/11	277	52	36	3.4	20	2500	520	710	18	40
3/18	183	52	30	3.3	8	1600	530			
4/19	184	51	40	3.0	7	1500	500			
5/4	127	59	38	3.5	5	1400	515	577	32	150
6/14	177	62	28	3.6	6	1450	471			
7/1	182	65	40	3.5	7	1500	648	683	7	66
8/2	181	56	48	3.4	6	1450	677			
9/21	96	-	-	3.3	2	1100	471			
10/23	96	69	38	3.7	2	1100	481			
11/30	169	-	-	2.0	3	1200	500			
12/32	174	12	12	1.8	2	1100	560			

* see text for explanations

Ovalisation, determined as the difference between the maximum and minimum diameter measured at the same location, stayed generally between 30 and 40 µm with maximum values near 50 µm. The smallest ovalisation was measured for the ferritic pin where it did not exceed 12 µm.

3.1.2 Eddy current control /2/

Even though the eddy current signals of all the austenitic pins appeared very disturbed, which made the interpretation difficult, the French analysts concluded that only for pin 5/4 did the signal give indications of some notable corrosion at the fissile/fertile interface (RIFF - see fig. 3). For lower locations in this pin or in all the other pins there were only signals indicating weak or no corrosion. The signals for the ferritic pins were, in contrast to the austenitic pins, very monotonous and indicated no corrosion.

3.1.3 Radiography

All the pins were neutron radiographed in Cadarache. The pins examined in Karlsruhe also had betatron pictures taken. Both types of radiography enabled the fuel column elongation and the extension of the central channel to be determined. Since there are large discrepancies in the values for the central channel, both sets of measurements are given in table 4. For the fuel column elongations, the values obtained by betatron and gamma scanning were preferred over those determined in Cadarache.

Both types of radiography revealed a local enlargement of the central channel near the core mid-plane in each of the two pins with initially wide gaps. In these pins, the length increase of the fuel column was much larger than in all the other pins. In the pins with smaller gaps, including the annular pellet pins, dark areas in the central channel could be observed which appeared as local blockages.

3.1.4 Gamma spectrometry

Axial gamma scans on all 10 pins with removed spacer wires were supposed to have been performed in the LDAC/Cadarache, for the isotopes Zr-95, Nb-95, Ru-106, Sb-125, Cs-134 and Cs-137. Presumably scans were made of pins 1/8, 2/11, 2/8 and 12/32. Available for this report were only those gamma profiles given in /2/, which are reproduced in fig. 5, 6 and 7. Later, in Karlsruhe, gamma measurements were made on pins 2/11, 5/4, and 7/1. Since Zr/Nb-95 had already disapppeared, meaningful scans were taken for the two caesium isotopes and Ru-106 only. Some of their profiles are reproduced in figs. 8 through 14. The profiles of the two

caesium isotopes were similar per pin, but showed significant differences from one pin to another. The general peaking on the fuel column ends was hardly discernible in the small gap pin. Besides the peaks at the ends, there were also areas of high intensities near the middle part of the fuel, especially in the wide gap pin at the position where the radiographs revealed channel widening (Fig. 10). At this location, a large dip in both the Ru-106 and the Zr-95 profiles indicated loss of fuel (Fig. 5, 6 and 14). In the other pins, the ruthenium intensity peaks coincided with dark areas in the central channels as seen in the radiographs.

3.2   Destructive examination

Destructive examinations were performed in the Hot Cells of KfK on only three pins of ALKEM fabrication. The three pins selected were pin 2/11 as representing the SNR Mark II type pin with a relatively large fuel-to-cladding gap and a smear density of 88 % TD; pin 5/4 equipped with a small gap and high smear density of 92 % TD; and pin 7/1 as an annular pellet pin. Their sister pins were foreseen for re-irradiation in the HFR.

3.2.1   Fission gas and free volume

The values obtained from fission gas and free volume measurements are given in table 3. Due to a malfunction of the fission gas adsober trap, the released fission gases of pins 2/11 and 7/1 could not be collected and escaped into the cell atmosphere. Only the gases of pin 5/4 were directly measured. However, the Kr-85 activity of the escaped gases of all three pins examined at Karlsruhe was measured which allowed a fairly reliable determination of the released amount of fission gases in the other two pins.

3.2.2 Ceramography

The aim of the ceramographic investigation was fuel behaviour, especially in pin 2/11 with the large local opening of the central channel near the mid-plane which was interpreted as local overheating, and in the annular pellet pin 7/1 to confirm fuel condensation on the column ends; fission product behaviour, especially the nature of the inclusions in the central channels seen in the radiographs; and inner corrosion.

The choice of cuts for each pin was made with the help of the radiographs and was not systematic, except for one cut at the position 430 mm from the lower fuel/fertile interface, which was decreed to be the maximum power position by

the person responsible for the pin sectioning. In reality, the position of maximum linear power was about 120 mm further below. Nevertheless, the power at 430 mm was only slightly less than the maximum, and the position was probably very close to the maximum fuel temperature. Hence, still a reasonably good choice. Another position that was ceramographically examined and common to all pins, was the upper fuel/fertile interface.

The repartition of the cuts for the pins is listed in table 5. The positions are given relative to the lower fuel/fertile interface. This table also lists the results of the measurements on the various cuts such as the diameter of the central hole and the columnar grain region, the residual fuel-to-cladding gap, and the depth of cladding attack. It is indicated whether the central channel is blocked or not by condensed fuel or fission product inclusions (metallic ingots). Some of the transversal and longitudinal cross sections are reproduced here. The cross sections taken just above the core mid-plane, at 430 mm from the lower fuel end of all three pins, are shown in figs. 15 to 17. The difference in fuel behaviour of the three types is evident, particularly by the autoradiographs as well as the polarized images in fig. 18.

Cladding attack remained insignificant in all three pins. Although material with the appearance of reaction products could be found all along each pin in the gap between and on the surfaces of fuel and cladding. These possible reaction products showed up as metallic particles, agglomerations and even in layers (fig. 26). Sometimes they were mixed with a ceramic looking material to give the appearance of the classical, so-called mottled zone.

Although there were corrosion products found in all cuts, reductions in wall thickness were measured only in those samples from or near the upper fuel/fertile interface. The deepest attack of 30 μm was observed in the annular pin at a single location near the interface. At other locations, an occasional penetration of 3 to 10 μm was detected, practically all within the upper 70 mm of the fuel column. In the wide gap pin 2/11, the attack did not exceed 10 μm, and in the narrow gap pin 5/4, it remained within 20 μm. No real penetrations were measured in the mid-plane, high linear power regions. Unfortunately, no cuts were made available from positions where cladding attack is normally found, i.e., about at 75 % of the fuel column height or halfway between the mid-plane and the upper fuel end. For these positions, the eddy current signals indicated, for pins 5/4 and 7/1 as for some others, weak attack of the so-called ROG type (see fig. 4).

Table 5: Results obtained from ceramographic investigation

PIN	Cut	Pos.	diameter		F.-cl. gap radial	Cladd. attack	Remarks
			cent. h.	col. gr.			
		mm	mm	mm	µm	µm	
2/11	L 1	380 ÷ 400	2.3 ÷ 3.6	5.4 ÷ 5.7	70 ÷ 130 (200)	0	
	L 2	400 ÷ 420	3.3 ÷ 2.1	5.7 ÷ 5.4	50 ÷ 150 (250)	0	
	T 3	430	2.1	5.4	60 ÷ 80 (300)	0	
	L 4	730 ÷ 750	pores	(4.0) restruct.	40 ÷ 130	0	
	L 5	750 ÷ 770	pores	(4.6) pores	70 ÷ 120	10	
7/1	L 1	0 ÷ 20	0 ÷ 0.5	3.2	60 ÷ 110	0	clogged
	L 2	115 ÷ 135	1.2 ÷ 1.5	4.8 ÷ 5.0	60 ÷ 100	0	clogged met. ingot
	T 3	430	1.8	5.2	50 ÷ 130	0	
	T 6	690	0.15	2.5	40 ÷ 140	0	clogged
	T 4	735	0.5	(4.2) restruct.	60 ÷ 100	0	clogged
	L 5	745 ÷ 765	0.6	(4.5) pores	80 ÷ 130	30	clogged
5/4	L 1	305 ÷ 325	0.4 ÷ 1.32	4.5	40 ÷ 70	0	clogged met. ingot
	T 2	430	1.32	4.7	20 ÷ 40	0	
	L 3	435 ÷ 455	0.9 ÷ 1.4	4.8 ÷ 4.5	20 ÷ 40	10	clogged met. ingot + fuel
	L 4	740 ÷ 760	pores	3	20 ÷ 140	20	

L = longitudinal cut, T = transversal cut

Some micro gamma scanning (MIGAS) activity was spent on cut T4 of pin 7/1 in order to investigate the bright spot in the centre of the beta autoradiograph in fig. 22. The investigation clearly showed that it was caesium and not ruthenium as normally expected with such bright spots.

4. Discussion

4.1 General

The results obtained from POUSSIX will be compared with those from MEDINA /4/. The MEDINA irradiation was used as a forerunner for POUSSIX. In MEDINA, only one pin was involved, which was made up of four fuel stacks, each one composed of pellets from the same fuel types and batches used in the ALKEM pins in POUSSIX. We had therefore the same variation in smear density and gap size, however, all integrated in one single pin. The irradiation took place in the Pool Side Facility (PSF) of the HFR in Petten, i.e., under a thermal flux as opposed to POUSSIX where we had a fast flux. The power history was different, too. In order to enhance FCMI, a cyclic operation mode was chosen for MEDINA with alternating periods of intermediate (70 %) and full power. The ramps in going to full power after a period at lower power were supposed to give the cladding an additional push by the fuel due to the thermal expansion of the hotter fuel. After 24 experimental cycles, a maximum local burn-up of 8.5 at % was reached. Maximum local linear power was 505 W/cm, which has to be compared with the 447 W/cm of POUSSIX. The maximum mid-wall temperature was 562°C, i.e., relatively low. But the maximum temperature position coincided with the maximum power position, so it cannot simply be compared with the maximum nominal cladding temperatures given for the POUSSIX pins, which were generally higher, but occurred at pin positions where the power was low.

4.2 Fuel Clad Mechanical Interactions (FCMI)

The results of most interest in this experiment were the diametral increases as a consequence of mechanical interactions between fuel and cladding. The expansions given in fig. 3 for the austenitic pins were to a great extent caused by clad swelling. In the lower part of the fuel, where the cladding temperature was in the range of 400 to 470°C, swelling accounted for about 50 μm ($\hat{=}$ 0.66 %) of the diametral increases. This value can be derived from the pin extensions given in table 4. On subtracting the 50 μm from the values measured at the bottom of the fuel column (where the maximum swelling occurred) leaves very little diametral change due to the mechanical interactions. Further up the pin with increasing temperature, swelling became less important and the diametral

increases can be attributed to mechanical interactions. At the position of about 400 to 450 mm from the bottom of the fuel column (see fig. 18) where the cladding temperature was about 560 to 580°C, a differenciation of the cladding strains is possible. It is clearly shown that FCMI is primarily a function of the fuel-to-cladding gap. The smear density plays a secondary role. A diametral gap of about 100 μm produced a diametral increase of some 60 μm, and a gap of 180 μm an increase of around 30 μm, which is still large when compared to the cladding expansion measured on the ferritic pin of less than 10 μm in the same position or when compared to the expansion the MEDINA pin experienced over all four fuel stacks.

The fuel column in MEDINA with a diametral gap of 120 μm produced a diametral increase of 15 μm, here it was 50 μm. What we observe is that in POUSSIX the diametral increase is generally more important than in MEDINA, especially for small gap pins, even though MEDINA was run in a cyclic power mode which was supposed to bring about more FCMI. Since cladding swelling cannot be made responsible for these differences in the upper pin positions, we have to resort to in-pile creep of the cladding material for an explanation. In-pile creep thrives on dpa, which were more available in the fast flux of PHENIX than in the thermal flux of HFR. This means that in POUSSIX, the 1.4970 cladding deformed due to the pressure of the fuel at a stress lower than the yield strength. In MEDINA, on the other hand, it needed to go beyond the yield strength to deform the cladding. This situation is revealed by the micrographic pictures of the fuel cross-sections. The MEDINA fuel exhibits crack patterns in the outer (colder) fuel region that are typical of strong mechanical interactions (see fig. 26). In POUSSIX, these crack patterns are practically absent in the pins with a diametral gap of 180 μm and more, and also less pronounced in the small gap pin.

From the deformation profiles in fig. 3, it cannot be concluded that there was cold FCMI, i.e., cladding strain produced at the fuel column ends on cooling at reactor shut down. The gamma scans and the beta pictures indicate caesium accumulations on both sides of the fuel column with a preference on the cold end, and the least accumulation for the low gap pin. These accumulations apparently have not produced a particular fuel or blanket material swelling that was capable of deforming the cladding on cooling. However, for an evaluation of cold FCMI, it must be remembered that the fuel was initially fairly substoichiometric. Caesium-fuel and -blanket interactions need a lot of oxygen, which was probably not sufficiently available even after a burn-up of nearly 10 at %. As it appears from ceramography, the caesium was present in a

condensate of fission products, the so-called JOG, rather than a reaction product with the fuel or blanket material.

A very sensitive indication for early fuel/clad contact is the residual fuel column elongation, or rather its absence. The reason behind this elongation is differential thermal expansion of the fuel and cladding. It is mostly neglected as an FCMI indicator or dismissed as irrelevant, probably because of a lack in reference data. The variation in fabrication conditions, e.g., the gap size in POUSSIX, led to distinctly different fuel axial expansions (see table 4). The columns in the two pins with the wide gaps apparently could freely expand during the first heat-up phase. The measured elongation value of 20 mm corresponds to a fuel expansion at 2500°C, if one assumes equal fuel and cladding contraction on cooling of the pin to the PIE state. The fuel columns with smaller gaps between them and the cladding were hindered in their expansion by an early fuel/clad contact. For the same assumption as above, this happened when the inner fuel temperature reached 1400 to 1600°C for the German pins, and already at about 1100°C for the very small gap Belgian pins as well as for the two ferritic pins. The inner fuel temperatures that led to fuel/clad contact and stopped the fuel movement are listed for each pin as "effective temperature" in table 4.

Ovalisation can normally be considered as an FCMI indicator. However, for wire-spaced pins, as was the case here, ovalisation is most likely the result of spacer/cladding interactions, especially if the irradiation was by a fast flux and the materials were prone to swelling.

4.3 Fuel behaviour

Two features revealed an interesting fuel behaviour: first, the closure of the prefabricated central hole in the annular pins, and second, the widening of the central channel in the large gap pins which gave rise to the assumption that there was a hot spot or local overheating of the fuel. Let's look into the latter first.

As we have learned in the preceding chapter, the fuel columns in all but two pins established contact with the cladding on the first rise to power, and the cladding kept them in place during further operation. The exceptions were the two large gap pins. Here, the pellets moved freely during the whole heat-up phase and took advantage of the full possible thermal expansion. They got stuck during high power operation and the upper part was kept in place on the following cool-down cycle. The middle and lower parts retreated (where the relative

differential fuel shrinkage was the greatest) and opened up a pellet interface somewhere above the core mid-plane. This was not fully closed by thermal expansion on the next heat-up cycle, because, in the meantime, the fuel had come much closer to the cladding and contact was established before the fuel had reached a high temperature, just as was the case in the low gap pins on start-up.

For the neighboring hot inner fuel region, the pellet separation was like a large crack which had to be healed. It became the dumping site for all the nearby evaporating material, especially from the hot central channel. Permanently losing material to fill in the interpellet opening, the central channel widened and took the form of a spindle with the pellet interface in its centre. This shape near the middle of the fuel column provoked the French examination team (and not only them) to believe in an overheating. However, no indication from metallographic examination supports this belief. On the contrary, this was always a relatively cool spot for all materials in the vapour phase. Here we find not only condensed fuel but also large amounts of volatile fission products. As the gamma profiles (fig. 10) and beta pictures (fig. 24) reveal, there is at this position an accumulation of caesium. Hence, there was no evaporation of fuel and fission products away from but condensation of these materials into this position, with, of course, these materials coming from hotter sites nearby or further away, which is well demonstrated by the superposition of the gamma scans for Cs-137 and Ru-106 over this region in fig. 25. Unfortunately, pin cutting was planned and performed in such a way that the most interesting piece was cut out of this pin region. The cutting wheel was 1.5 mm thick. This is the space between the two longitudinal cuts shown in fig. 24 which included the location of the open pellet interface as indicated by fig. 25.

There are further arguments against the notion of an overheating in the wide gap pins. Firstly, there was initially about 5 % less fuel in these pins than in the lead pin 5/4, which furnished them with the lowest power level of the whole experiment. Secondly, the start-up procedure with a reduced power during the vaccination period and the two reactor cycles at only 2/3 of full power were such that restructuring and partial gap closure was well advanced before the pins could reach full power and consequently high fuel temperatures. By that time, the effect of the wide gap on fuel temperature was mitigated and little chance remained for overheating. Considering these arguments and the observations on fuel and fission product behaviour, there is no sound reasoning that speaks in favour of an overheating in these two pins. By the way, the wide central channel

in the upper column of the MEDINA pin was also blamed at first sight by some fuel specialists on overheating. Its real cause was also irreversible fuel column expansion.

In the annular pellet pins, the cold spots, where the evaporating fuel in the central channel could move to, were both ends of the fuel column. As the radiographs and the ceramographic examinations disclosed, some of the pellets at both ends became full or almost full pellets. These findings confirm for long fuel stacks what has been observed in the MEDINA experiment for short stacks. The condensation sites obviously depend on the temperature of the channel wall. According to the behaviour in pin 7/1, the dew point of the fuel vapour was closer to the end of the fuel stack in the lower part of the pin than in the upper part. At the lower fuel/fertile interface, the one fuel pellet facing the blanket stack was completely full, the following pellets were only partly filled, with the central hole increasing upwards. At the upper interface, the fuel pellet facing the blanket was only partly filled, and the central hole decreasing downwards. Only the 9th pellet from the top of the stack was full. From there on, the central hole increased again. There was no fuel condensation (or at least none to speak of) in the prefabricated holes of the blanket pellets on both sides of the fuel column (see fig. 27). The fuel/fertile interfaces were cold enough to completely trap all the fuel species in the vapour phase.

It is interesting to see from the alpha autoradiographs in figs. 19, 21 and 22 that there is no difference in fuel composition between the original pellet and the condensate in the former hole as one would expect form the different vaporization behaviour of plutonium and uranium oxide. There is indeed no inhomogeneity across the contour of the prefabricated hole, even not in structure. The closure of the hole apparently happened during the early stage of operation when the evaporation of the fuel was concruent, and reactor operation was still long enough to allow for restructuring in the colder regions at the extrem ends of the fuel column.

It probably does not need much fuel transport to clog the two opposite ends of an annular pellet stack. A rough calculation shows that of the 600 µm that the inner hole of pin 7/11 increased at mid-plane positions during operation, about 100 µm were used for axial redistribution, or about 0.7 % of the fuel cross section. About this much fuel was taken out from the high power positions and carried towards the lower power positions at both fuel column ends, giving a little relief for pin operation.

Void volume redistribution is part of fuel behaviour since contrary to appearance it is not void volume up the temperature gradient but fuel down the temperature gradient that is being transported by migrating pores /5/. Since the fabrication conditions provided for the same initial repartitioning of the void volume as in the MEDINA fuel, a similar analysis of the final void volume redistribution is given in table 6. For comparison, the table includes also the data for those three MEDINA fuel types that correspond to the ones of the three POUSSIX pins.

As we see from table 6, there is no difference for the small gap fuel type between POUSSIX and MEDINA. There is the same size of the central channel and therefore also the same ratio of transferred void volume over the one initially available for transfer. The fact that the central channel had the same size in POUSSIX as in MEDINA leads us to assume that the additional volume created by cladding expansion did not bring about more pore migration.

There are differences for the other two fuel types. The largest is observed in the large gap pin. The central channel has become much bigger, and the apparent ratio for the transferred void volume is high. However, much of the volume of the central hole has not come from the inital void volume in the cross section. Some of it was provided by the freely expanding fuel described above. The expanding hot inner fuel region created wide open, wedge shaped cracks in the outer fuel part. These cracks introduced new void volume which was transferred to the centre during the healing process. There are still traces of the whole procedure to be seen in figs. 17 and 24. Hence, for the volume of the central channel in pin 2/11 at position 430 mm, we had three contributions: firstly, part of the initial void volume in the pores and the gap which was responsible for the extension of the inner hole to a diameter of between 1.6 to 1.65 mm (or 60 % of the channels volume), secondly, the additional void volume introduced by free fuel expansion which accounted for an additional 350 µm to the diameter (or 30 % of the channels volume); and, thirdly, fuel evaporation that helped in healing the open pellet interface as described above. The latter added the remaining 100 to 150 µm (or 10 % of the channels volume) to the final channel diameter of 2.1 mm (see table 5). A good impression about the whole difference in behaviour of the fuel with the wide gap in POUSSIX as opposed to MEDINA is obtained from fig. 26.

The difference for the annular fuel was minor. Practically all of the additional channel volume in POUSSIX over that in MEDINA is due to evaporation and transport to both fuel ends as described above. Some minor contribution by crack opening due to fuel expansion cannot be excluded.

Table 6: Void volume redistribution for POUSSIX

PIN		2/11	7/1	5/4
Fabrication:				
Pores	% TD	4	3.5	4
Gap	% TD	8	5	3.4
Inner hole	% TD	0	3.5	0
Total v.v.	% TD	12	12	7.4
Transferable v.v.	% TD	12	8.5	7.4
PIE at 430 mm				
Central channel	% TD	10	7.5	4
Cladding strain	% TD	0.7	0.9	1.5
Transferred v.v.	% TD	10	4	4
Not transferred v.v.	% TD	2 (2.7)	4.5 (5.4)	3.4 (4.9)
Transferred /transferable	%	83 (79)	47 (43)	54 (43)
Central chan. /total v.v.	%	83 (79)	62 (58)	54 (43)

v.v. = void volume; TD = theoretical density
Values in parentheses include additional volume by cladding strain.

Void volume redistribution for MEDINA

Column		II	III	IV
Fabrication:				
Pores	% TD	4	3.5	4
Gap	% TD	8	5	3.4
Inner hole	% TD	0	3.5	0
Total v. v.	% TD	12	12	7.4
Transferable v. v.	% TD	12	8.5	7.4
PIE:				
Central channel	% TD	6	6.8	4
Transferred v. v.	% TD	6	3.3	4
Not transferred v. v.	% TD	6	5.2	3.4
Transferred / transferable	%	50	40	54
Central chan. / total v. v.	%	50	57	54

The additionally acquired void volume by cladding strain, even though it could make up for the difference between POUSSIX and MEDINA, is not believed to have contributed to the channel formation in pin 7/1, as well as in the other pins. Hence, the values put in parentheses in table 6 are not relevant. It should also be noted that the figures given in this table for the transferred void volume and the ratio of transferred over transferable void volume are only apparent but obviously not true values in the case of pins 2/11 and 7/1, as we have learned from the above explanations.

Fuel restructuring, i.e., the structural evolution of the fuel in a pin, reflects the thermal situation. This, at least, is a commonly accepted position. A good impression about the extent of restructuring is obtained from the dimensions of the central channel. A large central channel is not the only result of high temperature but also of, and this is by far the more important factor, the available void volume. There is no fuel restructuring without transferable void volume in the pin. And the more void volume we have, the more restructuring we get. These facts are reflected by the appearence of the cross sections of the three pins shown in fig. 18, as well as by the length values of the central channels given in table 4. The wide gap pins had by far the longest central channels. This may not be entirely evident when looking at the neutron radiography evaluation. However, fortunately, we also have the betatron radiographs which appear to be more reliable. The values obtained from the latter were partly confirmed by ceramography.

Other features that describe fuel restructuring, such as the columnar grains region, are primarily dependent on available transferable void volume and secondarily on the fuel temperature. In pins with more void volume to be transferred, the border line of the columnar grains extends to regions of lower temperature than in pins with less void volume. The conditions for the POUSSIX experiment may not have been optimal to arrive unequivocally at these conclusions (this was the case in the GIGONDAS 3 experiment /6/). Nevertheless, the pins did behave that way.

The velocity of the migrating pores, which do the restructuring work, depends not only on temperature but also on pore size. Sintering pores, believed to contribute the most to restructuring, are generally smaller than pores spawned from cracks and pellet interfaces. Their restructuring is slower than that of the big pores generated at crack sites. Therefore, we often find columnar grains reaching much further out to the fuel's surface at crack locations than in neighboring fuel

regions with sintering pores only. Very small pores don't migrate at all. They wait until they are sufficiently sized before they start moving. All the features that led to these conclusions were also observed in the POUSSIX pins.

Judging from the alpha autoradiographs, there appears to be a slight plutonium enrichment around the central channel accompanied by a depletion in the columnar grain region in all three pins. On the other hand, there is also a tendency to some higher Pu-content in the outer fuel regions.

A peculiar feature is seen in some cross sections from the upper part of the pins, where higher alpha intensities appear in thin layers in the gap or on the fuel surfaces (Figs. 21 and 22). Higher alpha intensities indicate plutonium enrichment. These fuel layers have a distinctly different structure from the bulk material they are sometimes lying on. They give the impression of being condensed from the vapour phase (fig. 28). This impression may have some credit in high power positions, but it does not make sense when these layers appear in cold pin regions as, for example, that shown in fig. 29 taken from the uppermost fuel pellet in pin 5/4. This latter figure demonstrates that the layer has its own behaviour. It spans an axial heat-up crack into which it was partly pushed by mechanical interactions with the cladding. The alpha picture in fig. 29 reveals the same composition of the layer and the fuel. There seems to be no sensible explanation for the existence of these layers in all three pins. They appear practically in all cuts except for those from the very low end of the fuel columns. Very preliminary microprobe results revealed now that the fuel layers are rich in uranium but low in plutonium /3/. It is the outer rim of the pellet that is enriched in plutonium and thus responsible for the high alpha intensity in the autoradiographs. This being the case, the only possible explanation for the appearance of the fuel layers in the gap is indeed fuel evaporation and condensation. Fuel evaporates from the pellet surface and condenses onto the cold cladding wall. For a 20 % plutonium mixed oxide fuel the uranium bearing species become dominant in the vapour phase at O/M ratios above 1.92. This was certainly the case in POUSSIX. Hence, the layer forming material was rich in uranium and the plutonium was left behind in the pellet rim. This does not explain all the features seen in the alpha autoradiographs, but it gives, so far, the only plausible reason for the existence of these layers. Surprising, however, ist still the fact that the evaporation/condensation mechanism also worked in the small gap pin in the upper fuel column regions where the linear rating was fairly low and consequently the fuel surface temperature not very high.

4.4 Fission product behaviour

The values about fission gas release in table 3 should be ragarded as tentative. The mean burn-up was calculated from the peak burn-up value of 9.57 at % and the ratio of the maximum over mean fluence obtained from the PHENIX team. The mean burn-up value thus determined amounts to 8.16 at % and is considered to be the same for all the pins in the bundle. The released fission gases were measured for pin 5/4 only. However, the Kr-85 activities are available for all three pins examined at Karlsruhe. In evaluating the release rates for the other two pins it was assumed that the amount of released fission gases is proportionate to the respective Kr-85 activities. The calculated releases range from 65 to 69 %, which is not particularly high, but should be expected for this type of fuel and reactor operation. The most release occurred in the wide gap pin 2/11, which is in line with the observed fuel behaviour, i.e., restructuring. It is, however, somewhat surprising that the release in the annular pellet pin was the same or even less than in the small gap pin. According to the conception of fission gas release being influenced by pore migration, we should have had more release in the annular pin. As we learn below, the behaviour of caesium corresponded much more to this conception. It is possible, however, that the activity measurements in the air vent of the Hot Cells did not account for all the Kr-85 released from the annular pin.

There are differences in the axial caesium redistribution between the three pins. The most was observed in the annular pellet pin 7/1, and the least in the small gap pin 5/4. The wide gap pin 2/11 occupied an intermediate position. There are good reasons for these differences and this order. The small gap pin had a tight fuel-to-clad contact, its fuel surface temperature was therefore lower, and since little transferable void volume was available because of the tight contact, there was also less pore migration and caesium release. All these things make for little redistribution.

The annular fuel pin 7/1 had initially a larger gap, more void volume to transfer, the contact was less tight, and the fuel surface probably hotter, even though the power rating was lower due to less smear density. All these circumstances induce more redistribution. The wide gap pin 2/11 had the most void volume available, its fuel-to-clad contact was the least tight, the fuel surface temperature could have been higher than in the annular pin, nevertheless, the axial caesium redistribution was less pronounced. The reason for this was the cold spot by the

separated pellet interface in the middle of the pin which trapped a lot of caesium and left less material to travel to the far ends of the fuel stack.

It was surprising to find caesium in the central hole of cut T4 from the annular pin 7/1 (fig. 22). This sample was taken about 30 mm above the fuel blockage in the central channel and some 20 mm below the upper fuel/blanket interface. There should be no doubt that the caesium got there during operation and not after reactor shut down. It needs operating temperatures to get caesium moving. But how it got there is puzzling. A possible explanation is the following: after the prefabricated central channel became clogged in the upper fuel column by fuel condensation, the remaining upper piece of hole was cold enough to serve as a condensation site for caesium vapour available at the fuel/blanket interface. The interface region had an open access to the central hole. The beta image of the cut from that region (fig. 27) clearly reveals the presence of caesium not only outside the fuel in the gap but also in the inner hole of the fuel and the blanket.

Most of the caesium generated was in the fuel-to-cladding gap. At least this is what the beta pictures suggest. It was to a great extent well separated from the fuel, which leads to the conclusion that it was not present as a caesium-fuel-compound but rather as a fission product compound. If the above observation is true, it will mean that the fuel remained substoichiometric to the end.

One special feature of fission product behaviour in this test was the substantial amount of metallic inclusions in the central channels of the annular and small gap pins. Surprisingly, no such agglomerations were found in the large gap pin. The same observations had already been made in the MEDINA test. The mechanism leading tho these accumulations is pore migration. This has already been described elsewhere /4,5/. But why it happened in pins with less transferable void volume and not in those with more void volume is still up for speculation. It is certainly not a possibly higher fuel temperature, as tentatively hypothesized in /4/. It now appears to be the contrary: a relatively low fuel temperature in the outer parts of the columnar grains region in the wide gap pins. In these pins, the columnar grains reached radially further into the cold regions of the fuel than in pins with smaller gaps. It probably needs sufficient wetting of the fuel material by the metallic precipitates to have the inclusions dragged along by the migrating pores. The wettability between fuel and metallic materials increases with temperature. If there is no or insufficient wetting, the metallic inclusions are buried under the condensing fuel in the pores and left behind. There were definitely more metallic inclusions trapped in the fuel matrix of the wide gap pin

2/11 than in the narrow gap pin 5/4. The fuel of the annular pin 7/1 holds an intermediate position. Judging from the migrating pore activity as indicated by the pictures of the cross sections in fig. 18, the order should be inverse. Accepting the above postulated hypothesis about metallic fission product transport would imply, however, that, after the initial restructuring has taken place and the gap was at least partly closed, the average fuel temperature in the wide gap pins was lower than in the small gap pins. This idea will probably be hard for modellists to accept but is conform with observations about fuel and fission product behaviour. Anyway, what makes the appearance of metallic ingots in the central hole interesting in the case of POUSSIX is the fact that the prefabricated central channel in the annular pin was blocked not only by fuel condensation at the column ends but also by large metallic fission product ingots. The presence of large quantities of metallic ingots but relatively small amounts of ceramic fission products as precipitation in the central channel is also an indication that the fuel was substoichiometric over the major part of its operation.

4.5   Inner cladding corrosion or FCCI

The substoichiometry of the fuel could be a reason for the little cladding attack found in POUSSIX. However, in MEDINA we had the same fuel, but there were significantly more chemical interactions with the cladding even though the penetrations or wall reductions were not spectacularly larger. In MEDINA, the most attack was found along the column with the wide gap, and opposite the annular fuel. Wall reductions amounted to only 40 µm but the gap was entirely filled with reaction products both metallic and ceramic. Here in POUSSIX, reaction products were sparse, with surprisingly the least in the wide gap pin and consisting essentially of what looks like metallic ones (they are probably a mixture of cladding components and metallic fission products like palladium). Ceramic reaction products were practically absent, at least as far as the optical investigations could discern. The ceramic material in the gap appears to consist of a fission product condensate which the French call JOG, and only little, if any, oxide raction products.

In POUSSIX, the deepest penetration depth of 30 µm was found in the annular pellet pin. The eddy current signal indicated weak attack, which corresponds to observation. For the narrow gap pin 5/4, where a penetration of only 20 µm was measured, the eddy current signal was interpreted as medium attack. In comparison with the annular pin, the attack in pin 5/4 was overpredicted. To the credit of the eddy current technique, it must be said, however, that in the gap of

pin 5/4 the metallic reaction products formed a continuous layer on the fuel surface, well separated from the cladding (fig. 27), which obviously simulated magnetically more attack than the few corroded grain boundaries still integrated in the cladding wall of the annular pin. The penetrations into the cladding of the wide gap pin did not amount to more than 10 µm.

Both POUSSIX and MEDINA have shown that cladding attack can be limited to small penetration depths with the high density, fairly substoichometric OKOM fuel, at least up to a burn-up of 10 at %. It is very probable that this is also true for higher burn-ups. What makes a comparison between POUSSIX and MEDINA interesting is the conclusion that long fuel columns in fast flux operation provoke less cladding reactions than small fuel columns in a thermal flux (irradiated under cyclic power conditions, though).

5.   Re-irradiation in HFR

As mentioned before, the sister pins of the ones examined at Karlsruhe were planned to be re-irradiated in the HFR/Petten for a power ramping test. Due to circumstances, only two of them underwent this test. The three pins were inadvertently and irreversibly loaded upside down into their irradiation capsule in such a way that only part of the fuel columns were going to be covered by the reactor core. Consequently, it was decided to re-irradiate only the annular (8/2) and the small gap (6/14) pins and discard the wide gap pin 1/8.

Due to the build up of poisons, notably Sm-149, during the PHENIX irradiation, a pre-irradiation phase in the PSF of the HFR was carried out for poison burning. This took 24 days during which the linear power was kept at about 450 W/cm, the nominal rating in the PHENIX irradiation. Following this burn-up phase, the transient was performed, whereby a peak linear power of 700 W/cm was achieved, i.e., an overpower transient of more than 150 %.

The pins survived. Post test examination revealed that the transient did not do much harm, at least as perceived from the outside via gamma scanning and profilometrie. Unfortunately, destructive examination had to be cancelled due to a revision of KfK activites on spent fuel pins.

According to the spiral traces (Fig. 30 and 31) taken in the Hot Cells at Petten, there were no additional cladding deformations. The diametral profiles before and after the transient testing are practically identical. The large ovalities seen in

figs. 30 and 31 are typical of wire-spaced pins in fast reactors. They resulted from the PHENIX irradiation.

Also the original (after PHENIX) caesium redistribution does not appear to have been affected by the HFR irradiation. In comparing the gamma scans for the caesium isotopes taken after the transient (fig. 32 and 33) with those obtained from the sister pins at Karlsruhe, we would be hard pressed to find, over the 500 mm of the lower part of the pin covered by the examination performed at Petten, differences that go beyond those normally encountered between individual pins.

There was, of course, a new generation of volatile radio-isotopes. Iodine exhibits some, but only little, axial redistribution. It did not migrate beyond the part of the fuel column that was covered by the reactor. Perhaps, the iodine was trapped by the caesium already present from the pre-irradiation. Nevertheless, the behaviour of the volatiles indicates that the HFR test did not bring about high fuel surface temperatures, high enough to stir them up from their resting place in the gap. And this holds for both pins, the annular as well as the small gap pin.

6.   Concluding remarks

POUSSIX was an interesting experiment. It was even more interesting in the combination with MEDINA. From both experiments we can draw the conclusion that it is difficult to get significant cladding strain by FCMI if we have a strong cladding. In MEDINA, the 1.4970 cw steel provided for a strong cladding, but not so in POUSSIX. A strong cladding in POUSSIX was the dispersion hardened ferritic alloy DT2203Y05. Obviously, the fast flux renders the work hardened 1.4970 soft, as soft as the solution annealed 1.4988, for example, for which significant cladding strains due to FCMI were measured in HFR and MOL experiments, i.e., also in irradiations under a thermal flux. The pressure the fuel is capable of transmitting to the cladding even in operational transients like those in MEDINA rarely exceeds the yield strength of a cold worked 1.4970 steel, which amounts to 450 MPa at 500°C. But it probably attains the strength of the 1.4988, which is 180 MPa at the above temperature. A pressure within these values will induce in-pile creep of the fuel which brings about relief for the cladding in case of power ramps.

Even though FCMI does not seem to be much of a problem, there is an early fuel/clad contact in a pin under operation. This contact is very likely not uniform around the periphery of the pellets. At start-up, a pellet will be in contact on one side. As its temperature rises, it will crack and the outer fuel chunks are being

pushed towards the cladding on the previously open gap side. If the initial diametral gap was not too large before the pin has reached full power, the contact will be firm enough to keep the pellet stack in place over a good part of its length. This, at least, is what we have learned from POUSSIX. Larger gap pins need somewhat longer to get a sufficiently firm contact. Nevertheless, their gap closure speed in terms of distance covered by time is faster, because in wide gap pins, or, more generally, in a pin with more transferable void volume, the restructuring activities are higher. The reason for this is not a higher temperature, as it may appear, but solely the surplus in transferable void volume.

Fuel swelling is not necessary to get fuel/clad contact. In fact, fuel swelling has nothing to do with it. Hence, fuel-clad gap closure is, in essence, not a function of burn-up, but rather of pin operation and inner fuel temperature. Fuel swelling is not and therefore should not be regarded as a factor determining fuel pin behaviour. A hot fuel under a thermal gradient provides for totally different fuel and fission product migrating mechanisms than an isothermal fuel. There is practically a 100 % release of gaseous and volatile fission products from a restructuring fuel. Also, there is practically a 100 % precipitation of metallic fission products and the so-called ceramic fission products that form inclusions in the part of the fuel that gets restructured. This part represents at least 50 % of the total fuel. In pins with much transferable void volume, it is even more. If we consider that about 35 % of all fission products are gaseous or volatile, or have been in that state for a sufficient time to become released, and another 35 % are those that form metallic or ceramic inclusions and finally precipitate out, then there are not many left to stay in solution and make the fuel swell. There is even a deficit for fuel swelling in the restructured zone, a deficit that can make up for the possible surplus in the non-restructured part. It is, therefore, no wonder that fuel pellet contraction rather than fuel swelling was actually observed and reported /7/.

A fuel behaviour code should take into consideration that the temperature gradient in the fuel is a factor in its own right. Many transport mechanisms are running by a temperature gradient, and secondary manifestations of fuel behaviour, such as fission product release, fuel swelling and creep, are directly influenced by the gradient. These mechanisms cannot be described or simulated by subdividing a fuel cross section into concentric, isothermal ring regions within which the mechanisms obey temperature dependent correlations. Within the restructuring fuel zone, pore migration is the motor behind the mechanisms

which are responsible for fuel and fission product behaviour, and not thermally activated processes like diffusion.

One can tell a good fuel code from a "not-so-good" one by looking at the mechanisms it uses. If, for achieving fuel/clad contact, it relies totally or to a great extent on fuel swelling, it is a "not-so-good" code. If it uses volume and grain boundary diffusion for fission product release, it is also a "not-so-good" code. A good code relies totally on fuel cracking and relocation for gap closure, and principally on pore migration and cracking for fission product release.

Concerning the aim of the experiment, namely evaluating the performance of high smear density fuel, it can be said that high smear density fuel pins perform well. The better part of the high smear density is the high bulk density. A large gap, though, is not beneficial at all. It makes the fuel unstable with consequences similar to those known from our experience with low density fuel. The small gap was not detrimental at all. The behaviour of pins with a diametral gap of 120 μm was by far better than that of pins where the gap was 270 μm. If one takes the results of POUSSIX and MEDINA, one would rather opt for 92 % TD smear density than for 88 % TD, and for a diametral gap of 120 μm rather than for a larger one.

References

/1/   F. Gibiat, M. Gouas, J. Isnel; Note technique SECLHA/LDAC 89-2004, Cadarache, 20.4.19989.

/2/   H. J. Heuvel: POUSSIX, CEA/DEBENE Bestrahlungs-Experiment in PHENIX, Stabdesign, Spezifikationen und Fertigungsergebnisse.
INTERATOM 54.06693.4 (Mai 1985).

/3/   H. Kleykamp, report in preparation.

/4/   O. Goetzmann, Report on HFR Power Cycling Experiment MEDINA/POCY 02 KfK report 5217 (Sept. 1993).

/5/   O. Goetzmann, LMFBR-fuel pin behaviour, in: Fast reactor core and fuel structural behaviour, Proceedings, BNES, Inverness, June 1990, p. 1.
Also: Fission product behaviour in fast breeder fuel pins, J. Nucl. Mater. 188 (1992) 58.

/6/   O. Götzmann, Nachbestrahlungsbericht über GIGONDAS 2 und GIGONDAS 3 KfK internal report 32.13.04 P02 A (November 1993).

/7/   M. Tourasse, M. Boidron, B. Pasquet, J. Nucl. Mater. 188 (1992) 49.
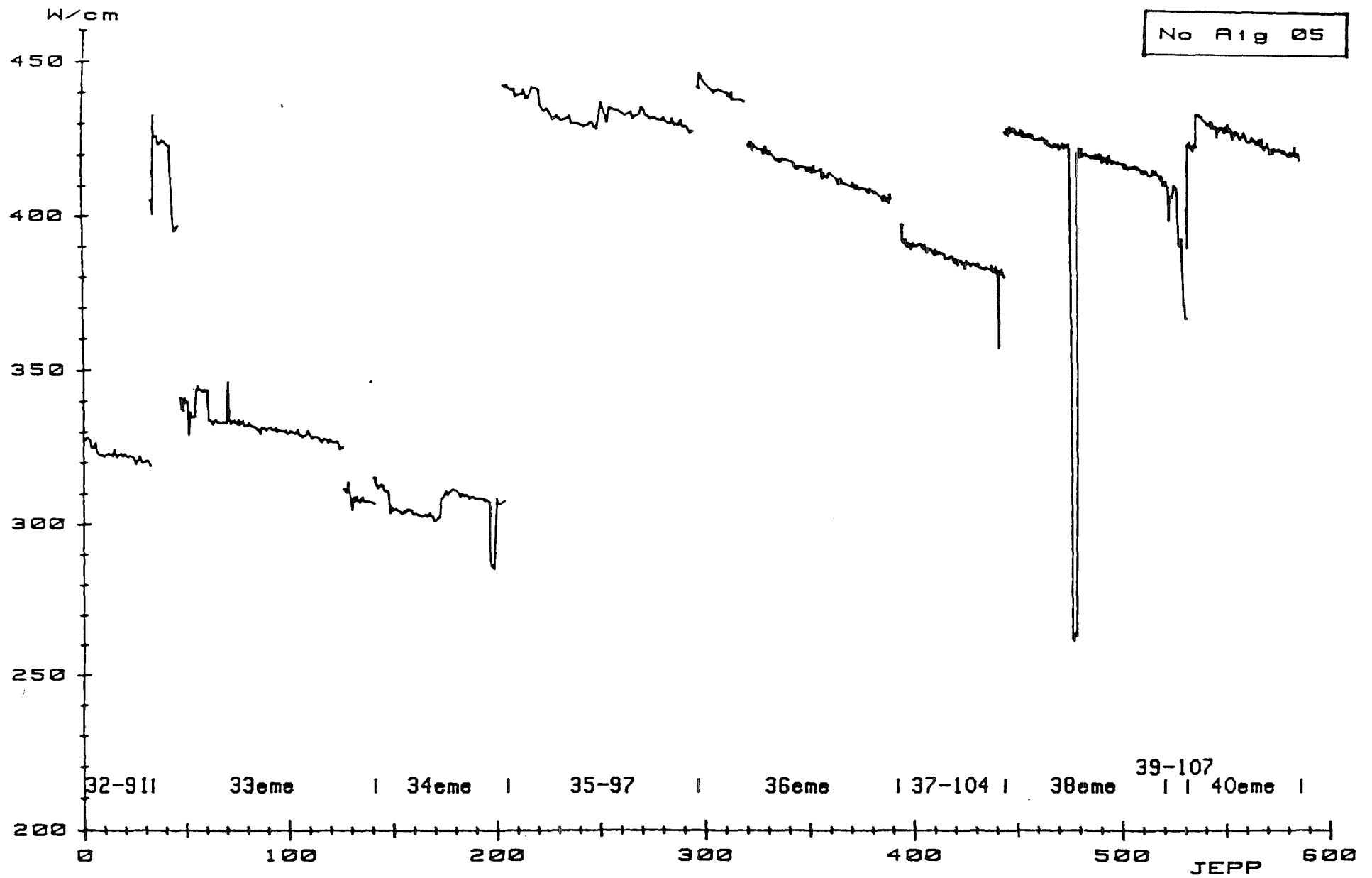
Fig. 1: Linear power history for small gap pin 5/4

TEMPERATURE GAINE DES AIGUILLES — POUSSIX [KCI 6503] 09/11/88

No aig 05
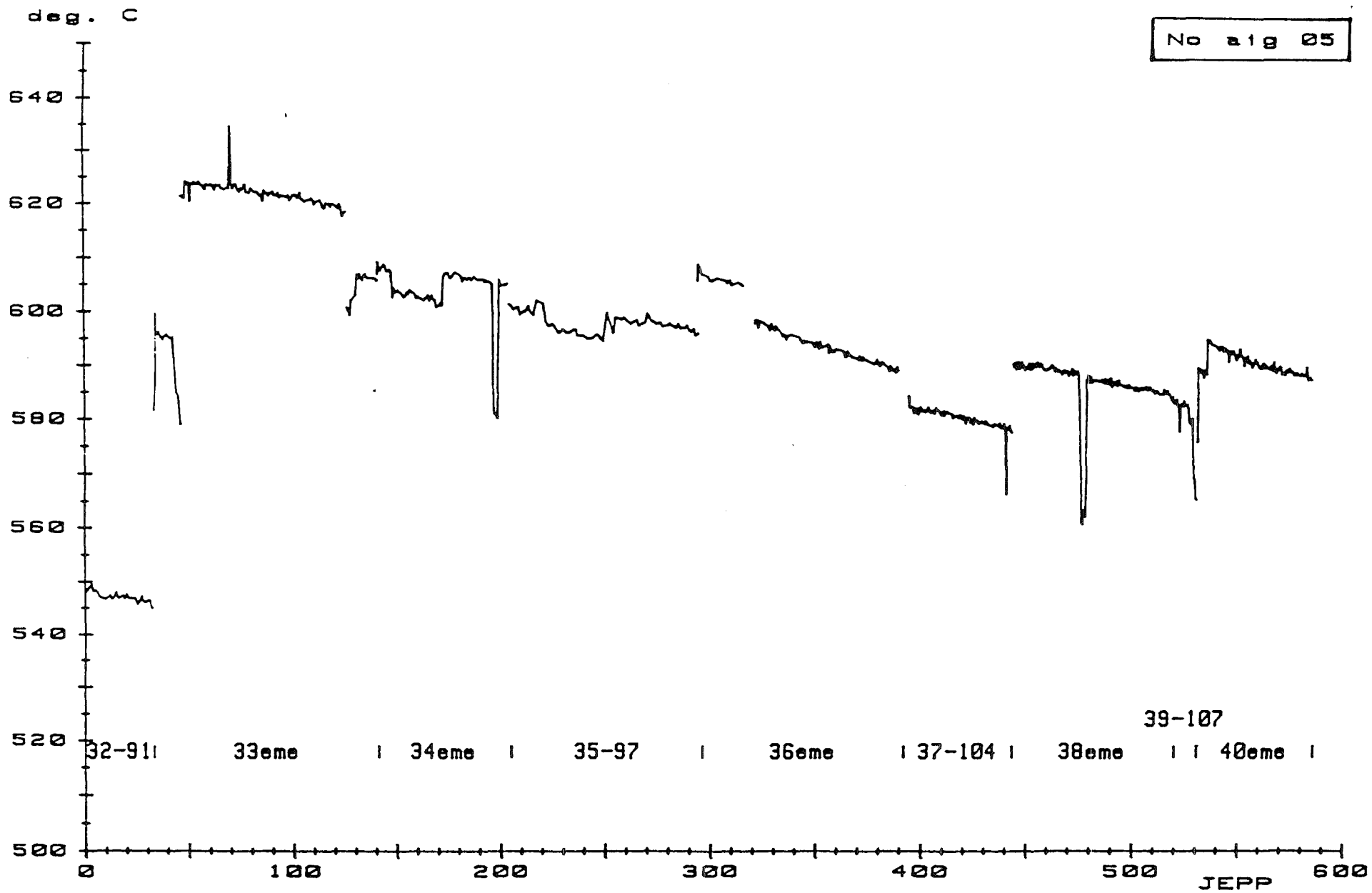
Fig. 2: Cladding temperature history for small gap pin 5/4

POUSSIX : Metrologies

	Jeu(µm)	%dth	dremp.
— 12 172	95.7	90.8
— 10 96	94.6	91.9
— 7-8 182+TC	96.6	88.0
— 5-6 120	96.	92.7
— 3-4 182	97.7	92.4
— 1-2 275	96.1	88.3
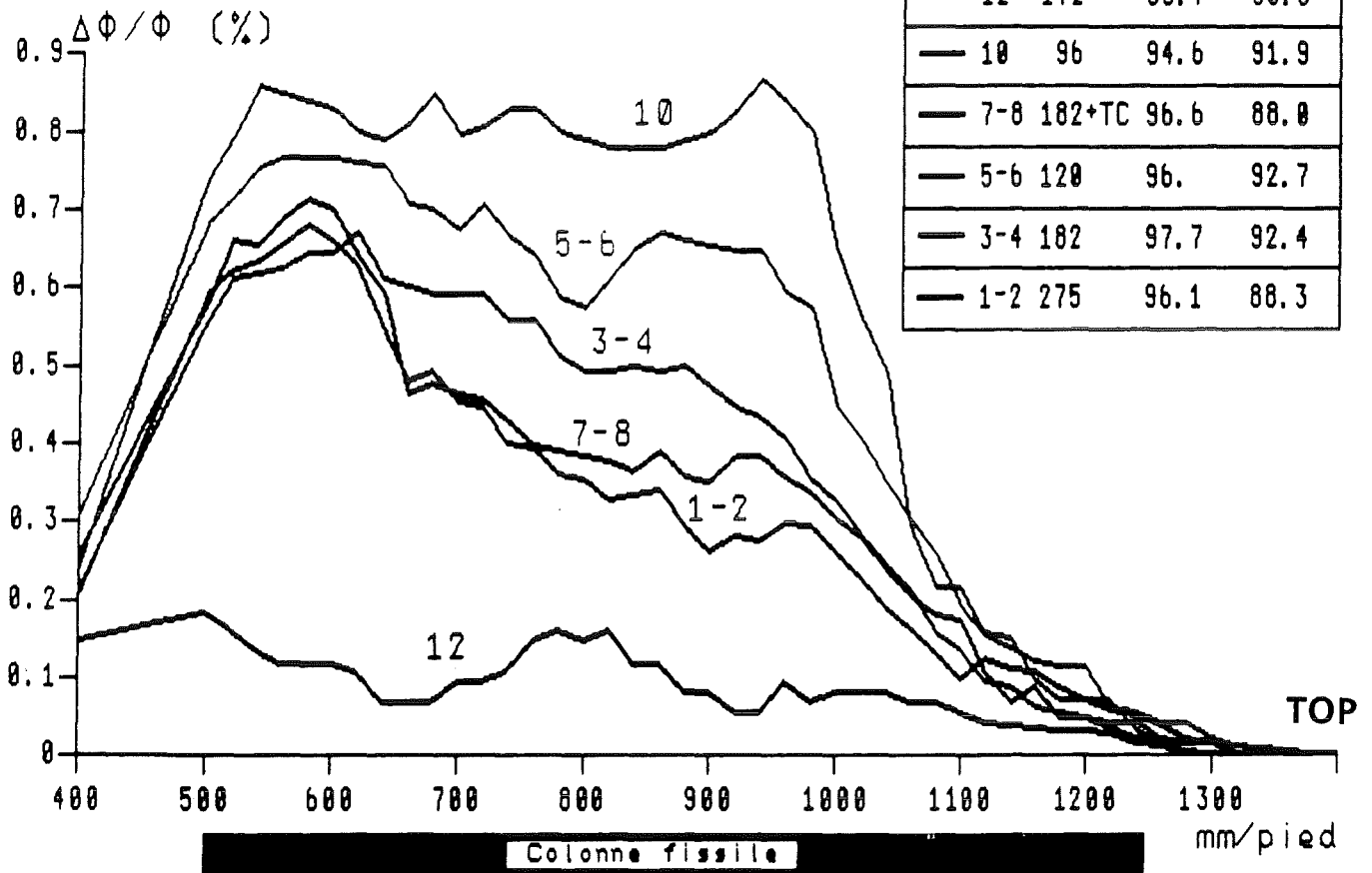
Fig. 3:   Axial diametral profiles of the pin types
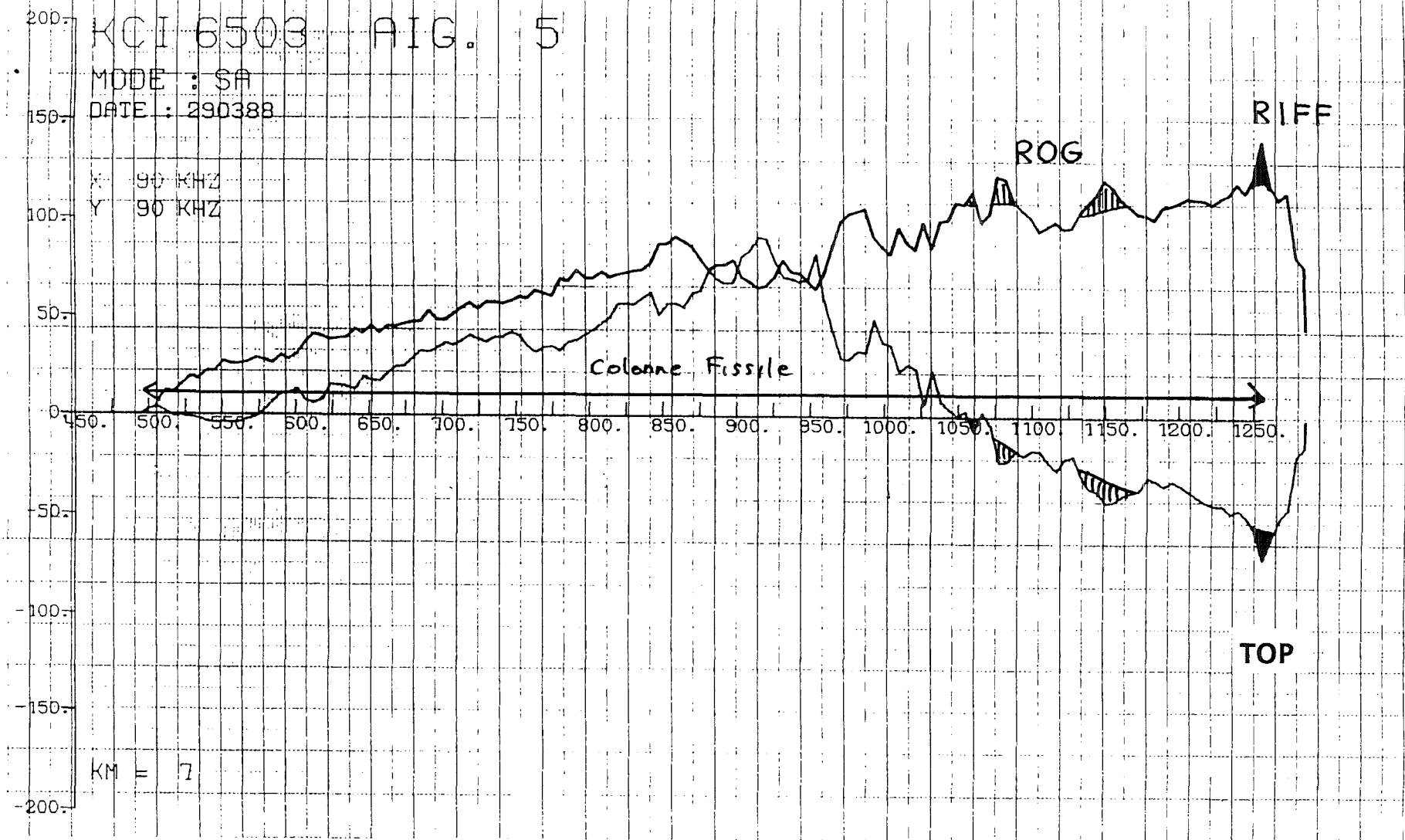
POUSSIX — Enregistrement CdF de l'aiguille 5 (Pou 04)

Fig. 4: Eddy current signal trace along small gap pin 5/4
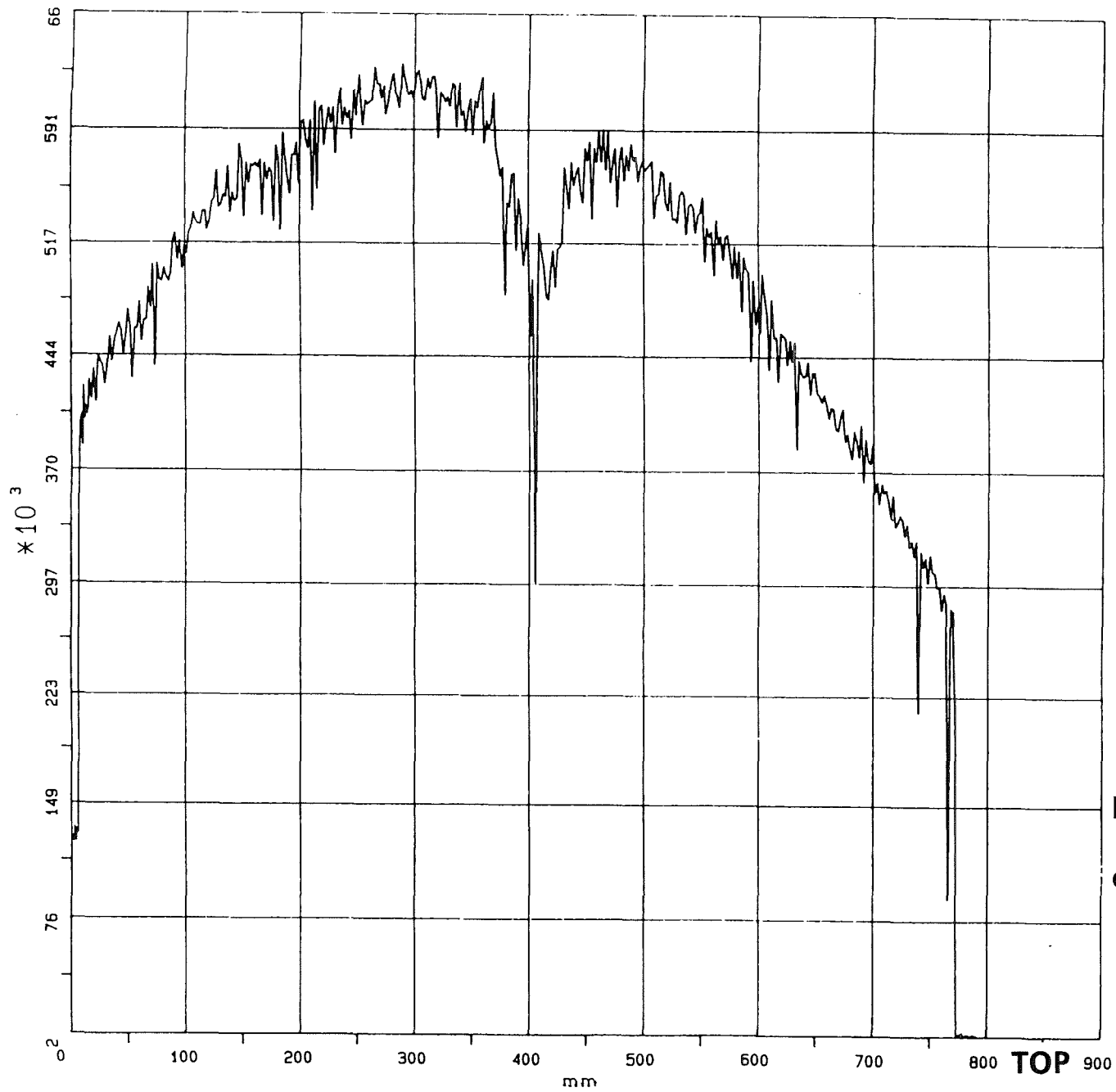
KCI 6503   POUSSIX

AIGUILLE   : 002

Nucleide   : Zr 95

Activite max : 6.33 10^5

Fig. 5:   Axial γ-scan for Zr-95
of large gap pin 2/11 (LDAC)

SPECTRO   LDAC
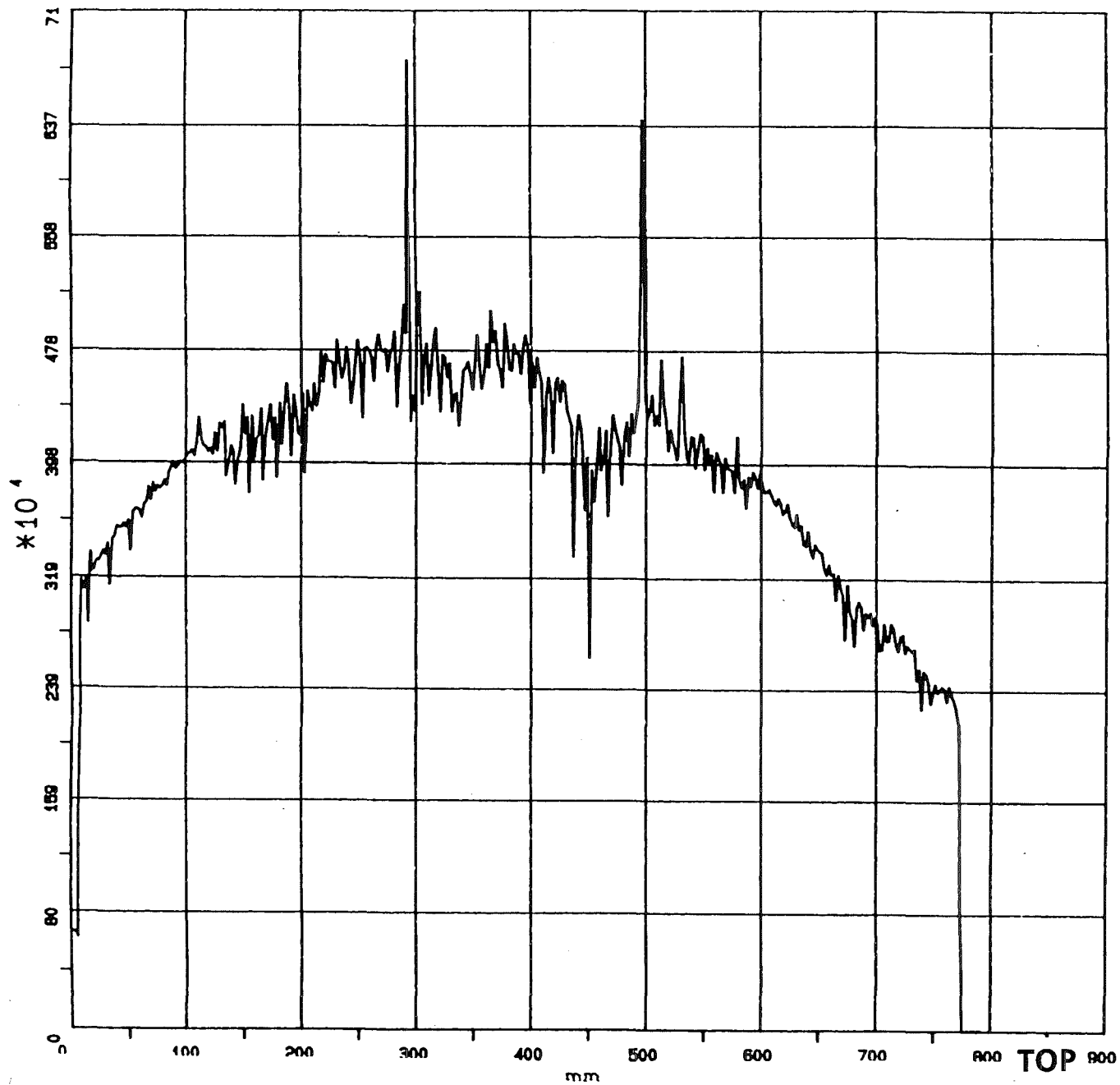
KCI 6503 POUSSIX

AIGUILLE : 001

Nucleide : Ru 106

Date : 03/10/88

Activite max : 6.83 10^{6}

Fig. 6: Axial γ-scan for Ru-106 of large gap pin 1/8 (LDAC)

SPECTRO LDAC
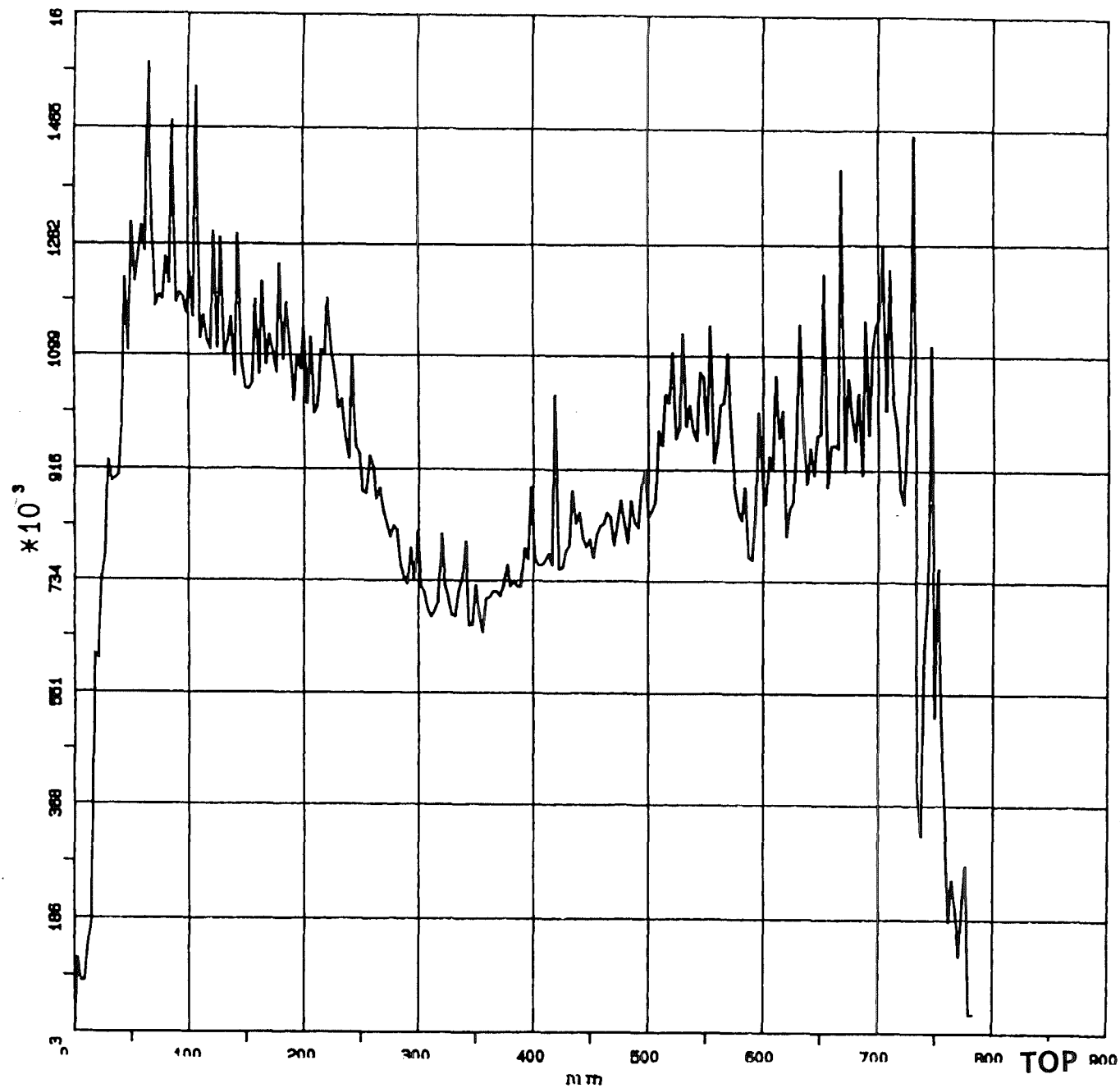
KCI 6503   POUSSIX

AIGUILLE   : 012

Nucleide   : Cs 137

Date   : 05/10/88

Activite max : 1.57 10⁶

Fig. 7:   Axial γ-scan for Cs-137
          of ferritic pin 12/32 (LDAC)

SPECTRO   LDAC
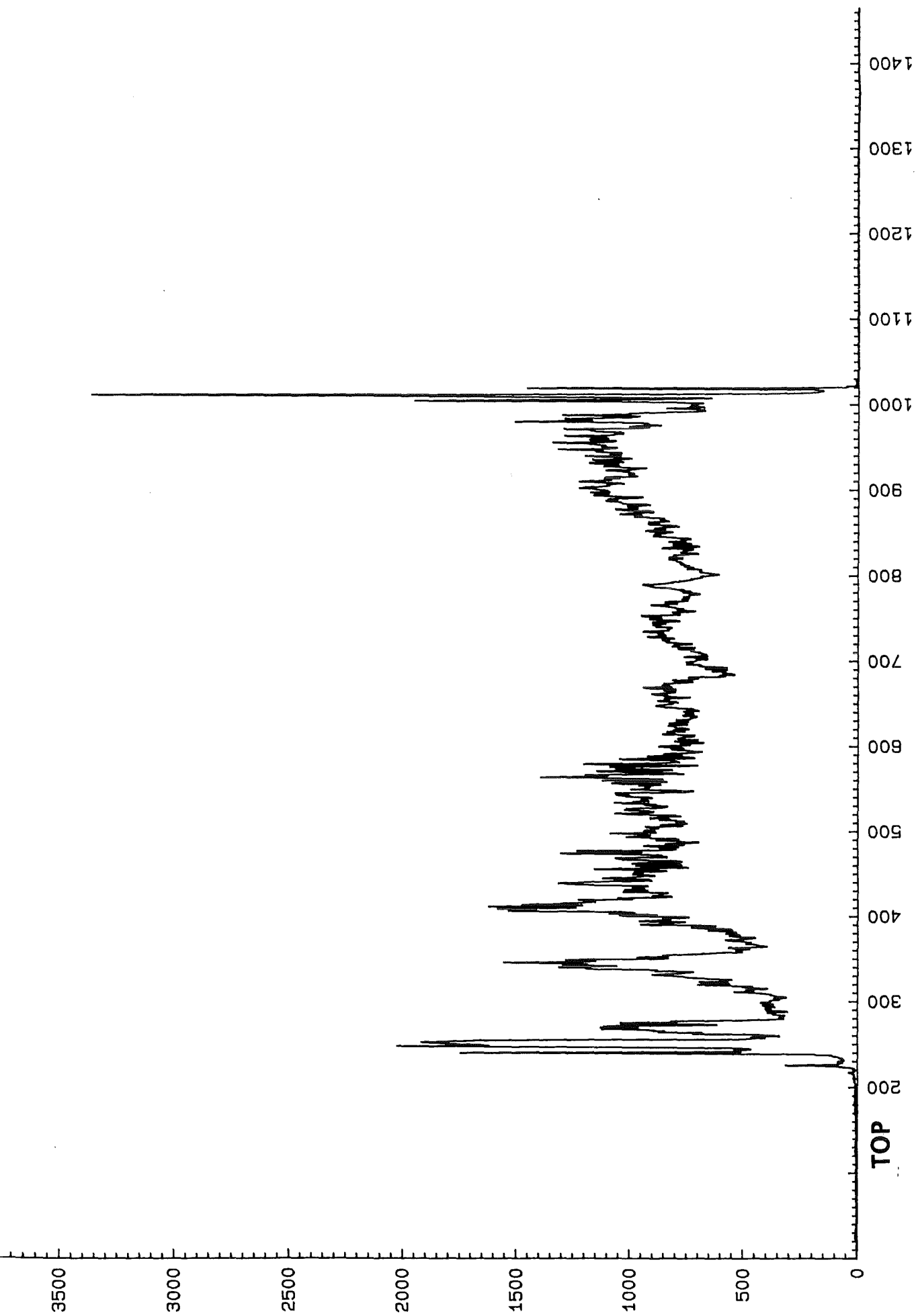
Fig. 8: Axial γ-scan for Cs-137 of annular pin 7/1
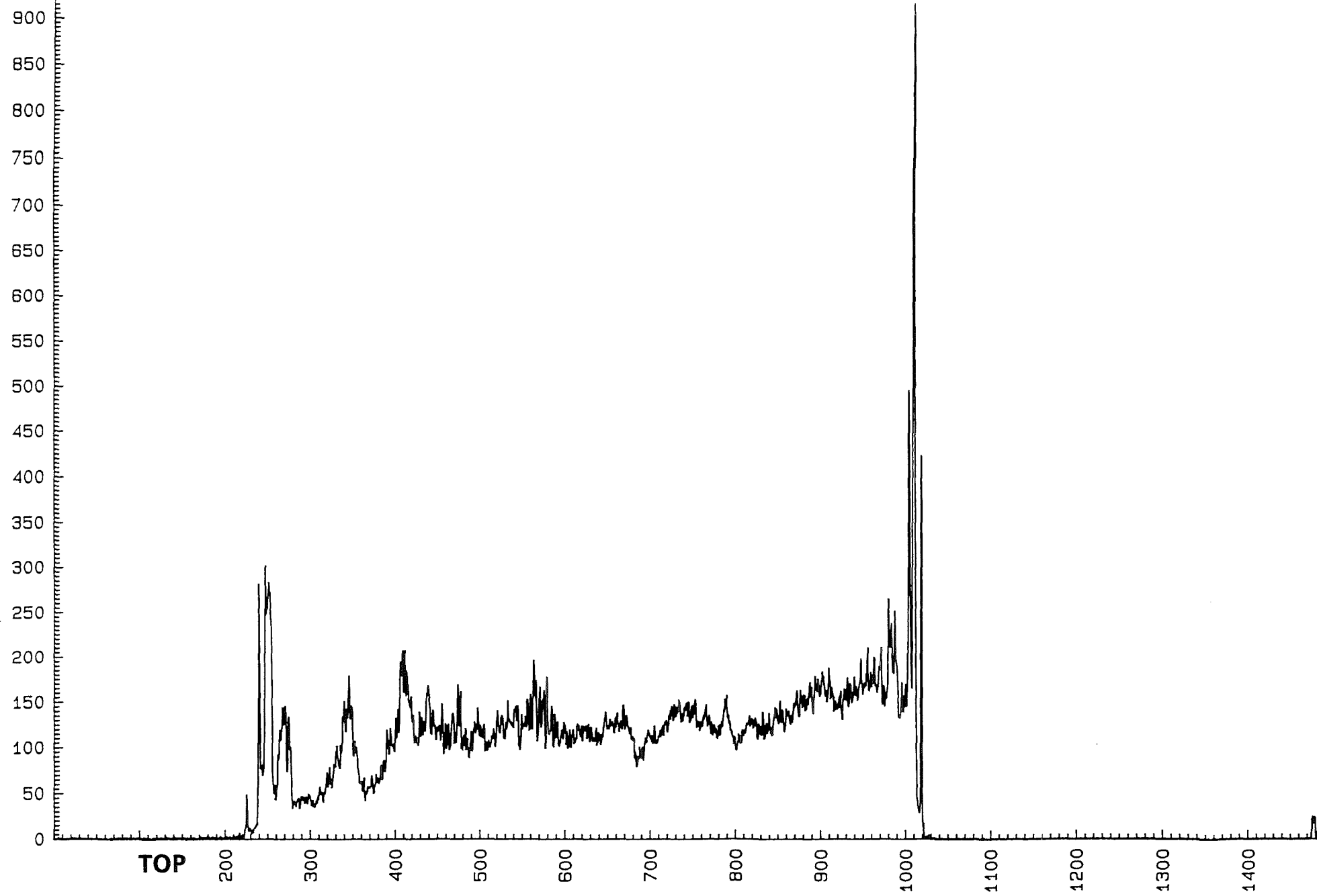
Fig. 9: Axial γ-scan for Cs-134 of annular pin 7/1
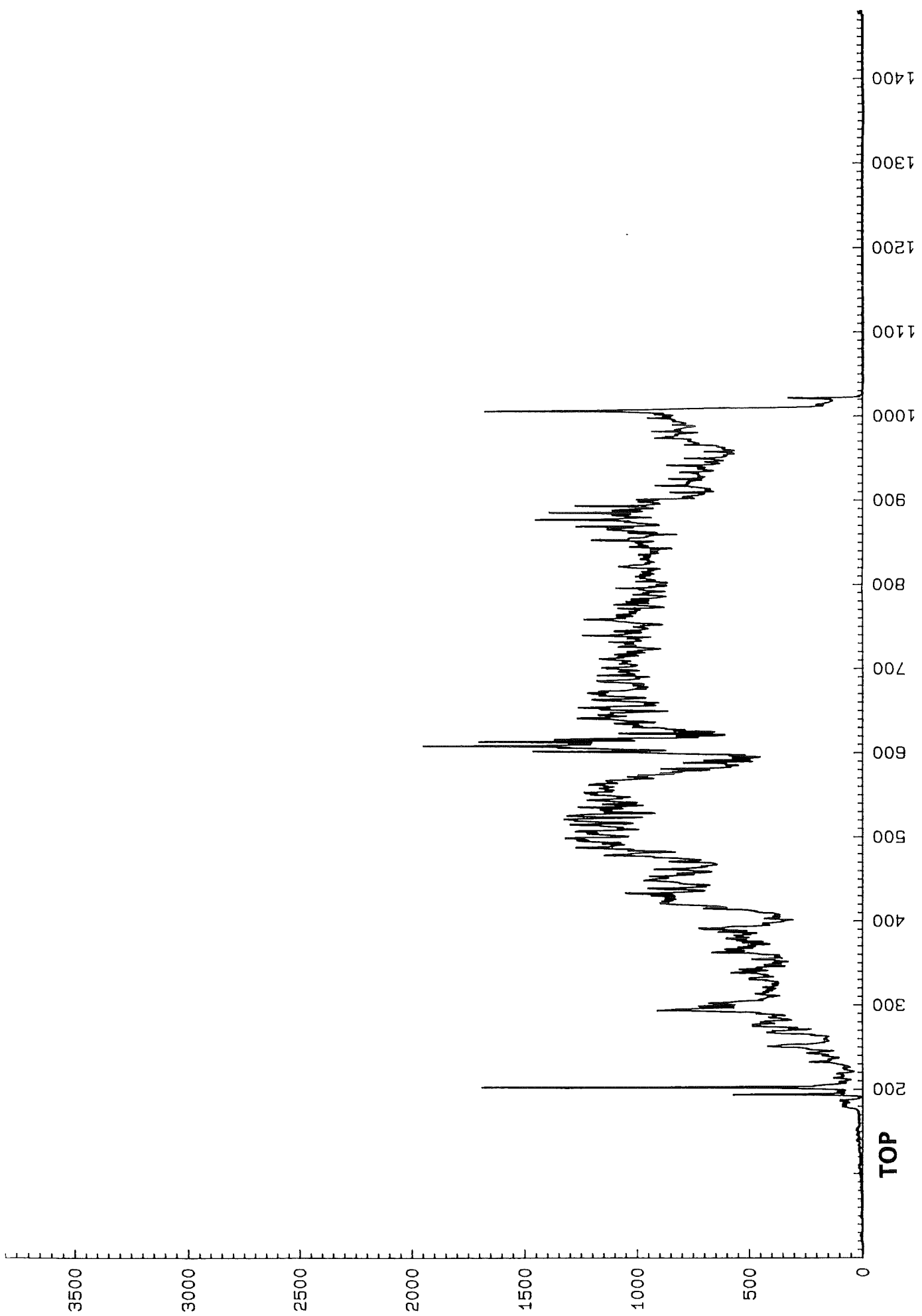
Fig. 10: Axial γ-scan for Cs-137 of large gap pin 2/11
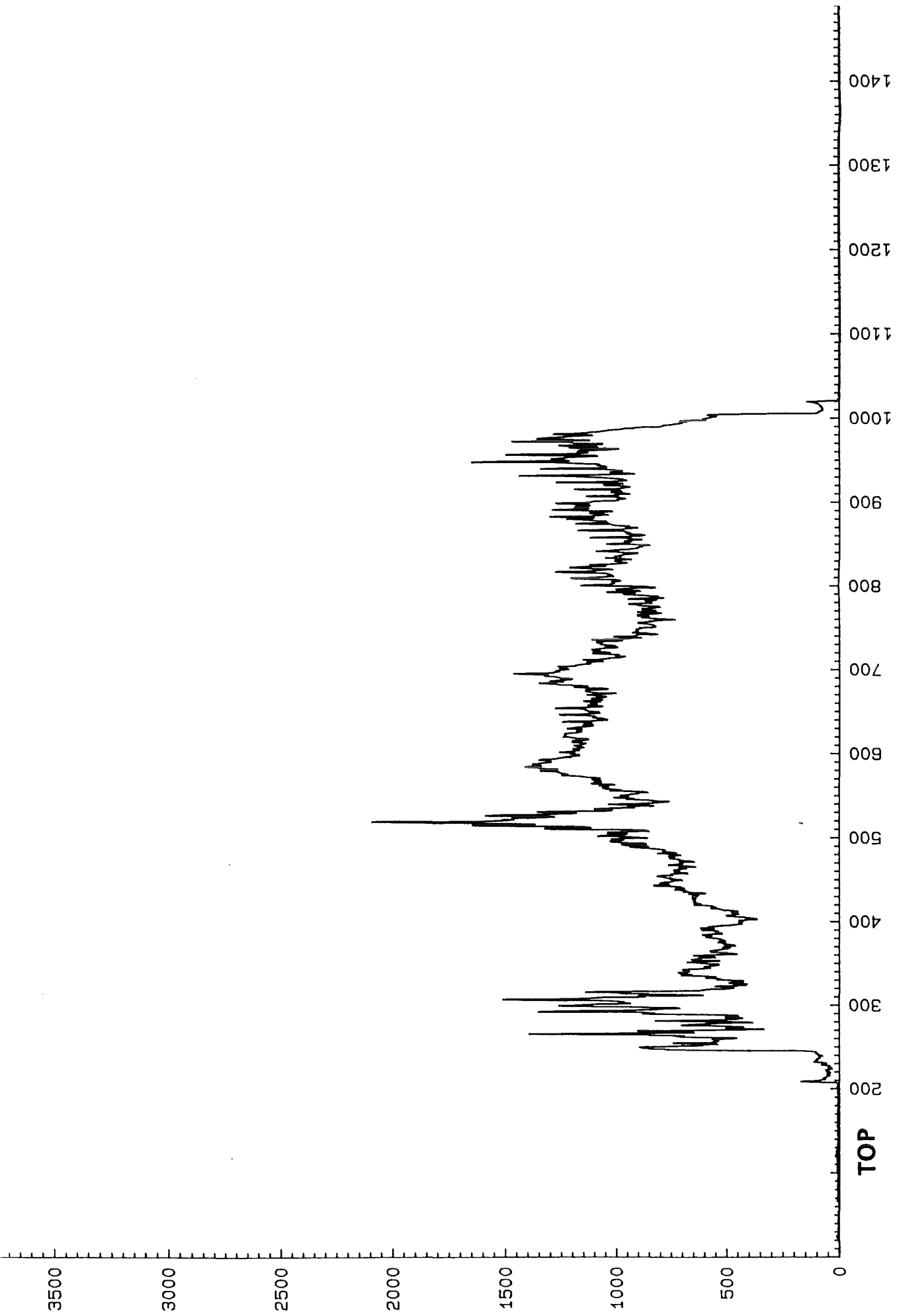
Fig. 11: Axial γ-scan for Cs-137 of small gap pin 5/4
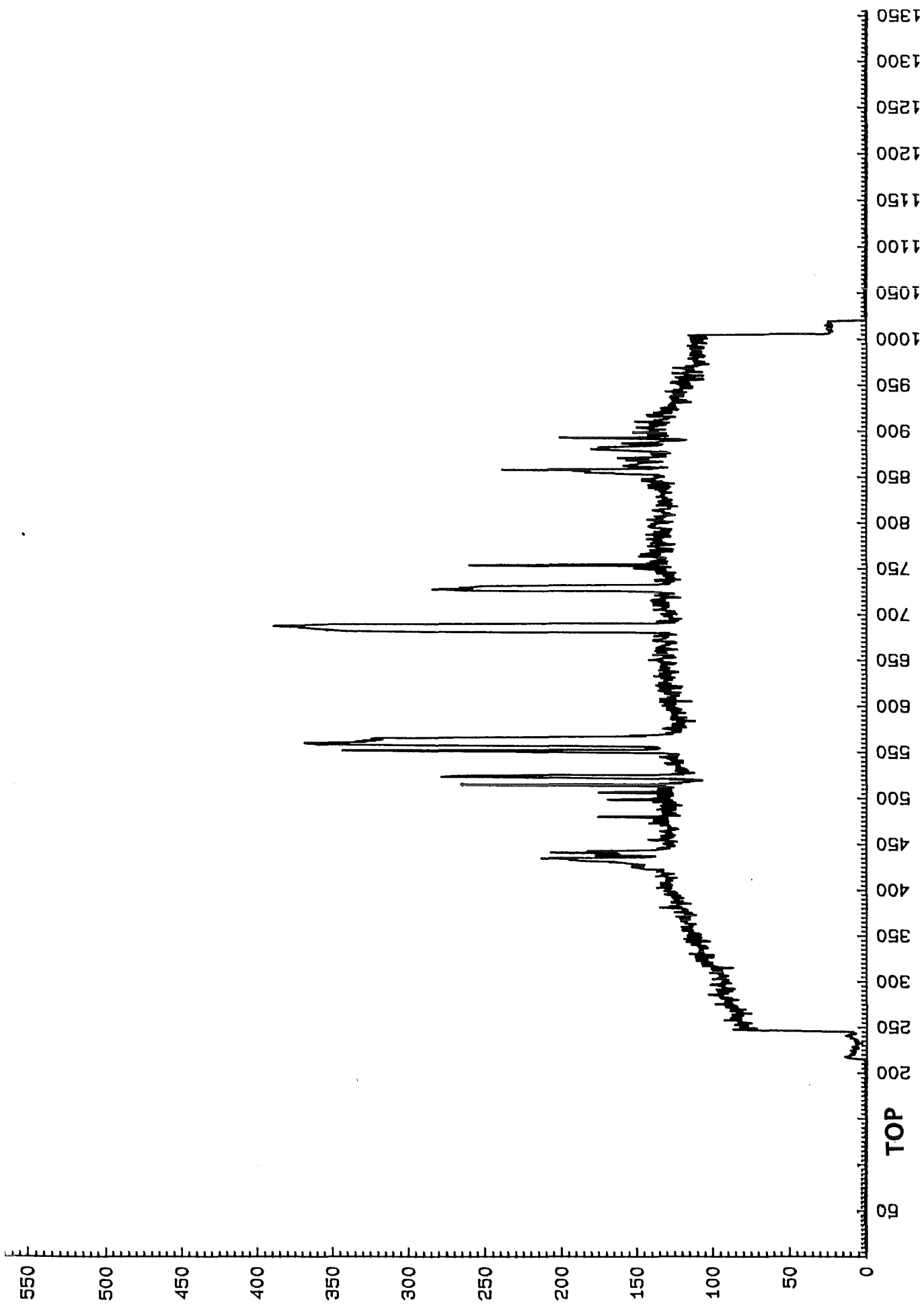
Fig. 12: Axial γ-scan for Ru-106 of small gap pin 5/4
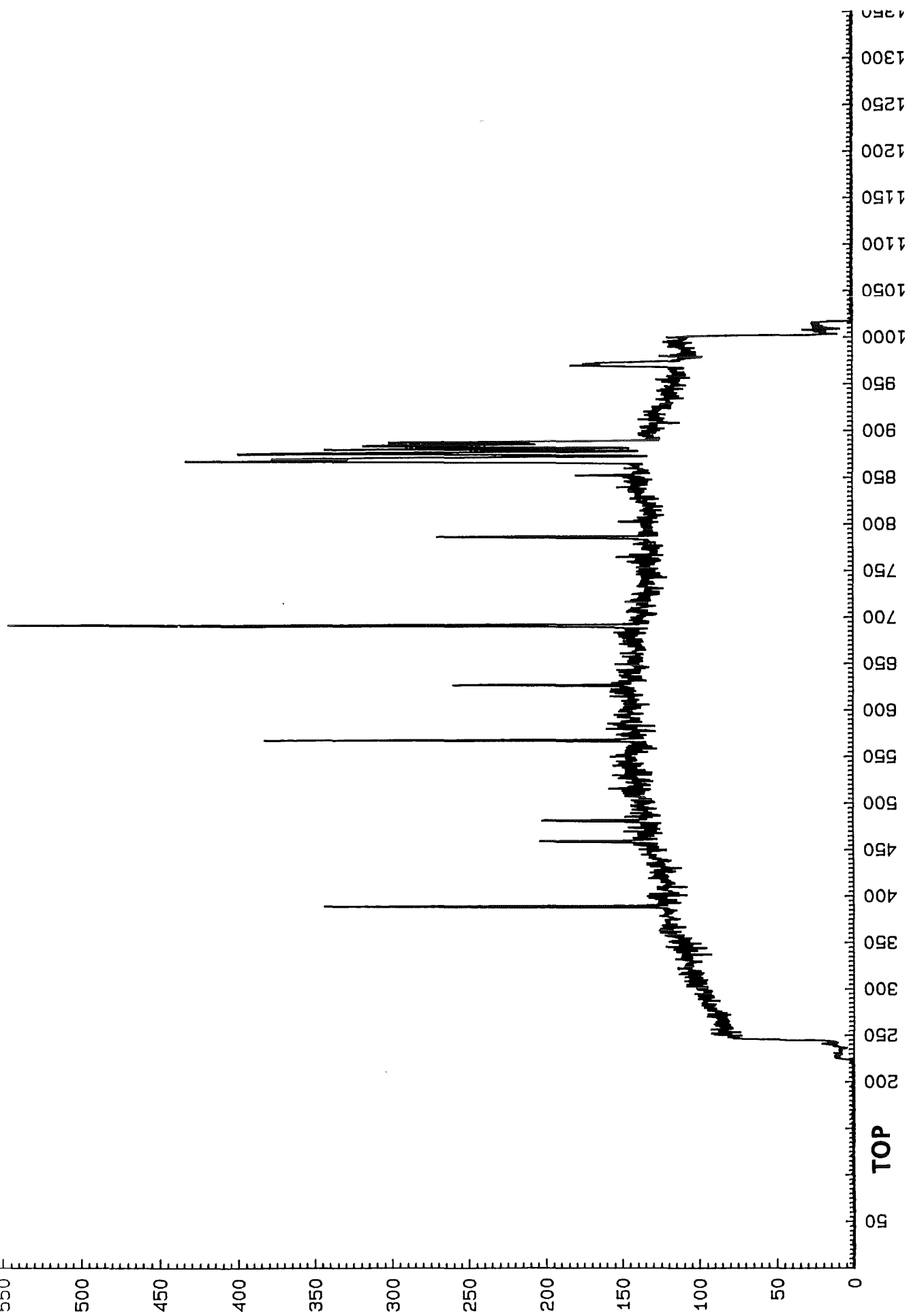
Fig. 13: Axial Y-scan for Ru-106 of annular pin 7/1
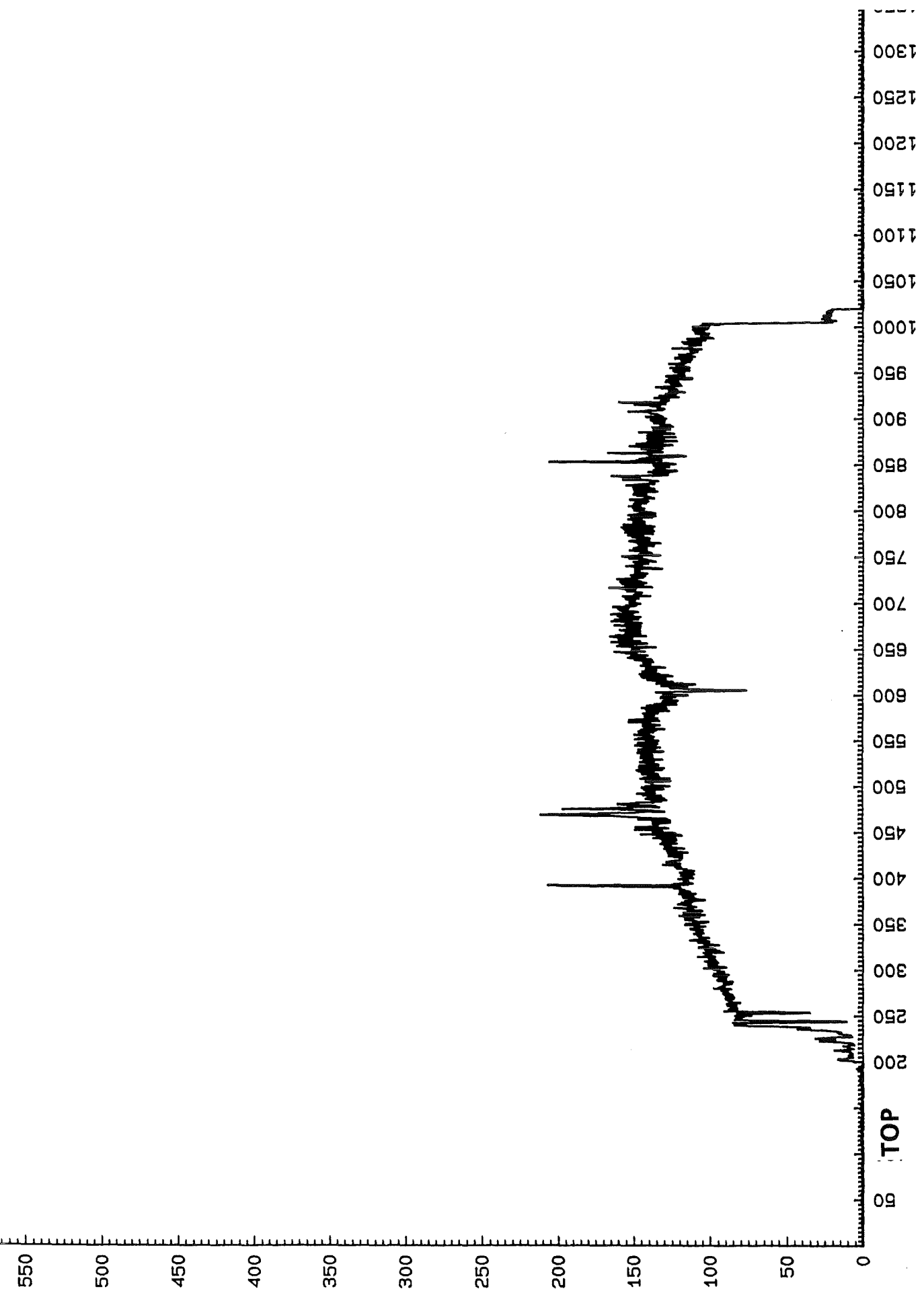
Fig. 14: Axial y-scan for Ru-106 of large gap pin 2/11
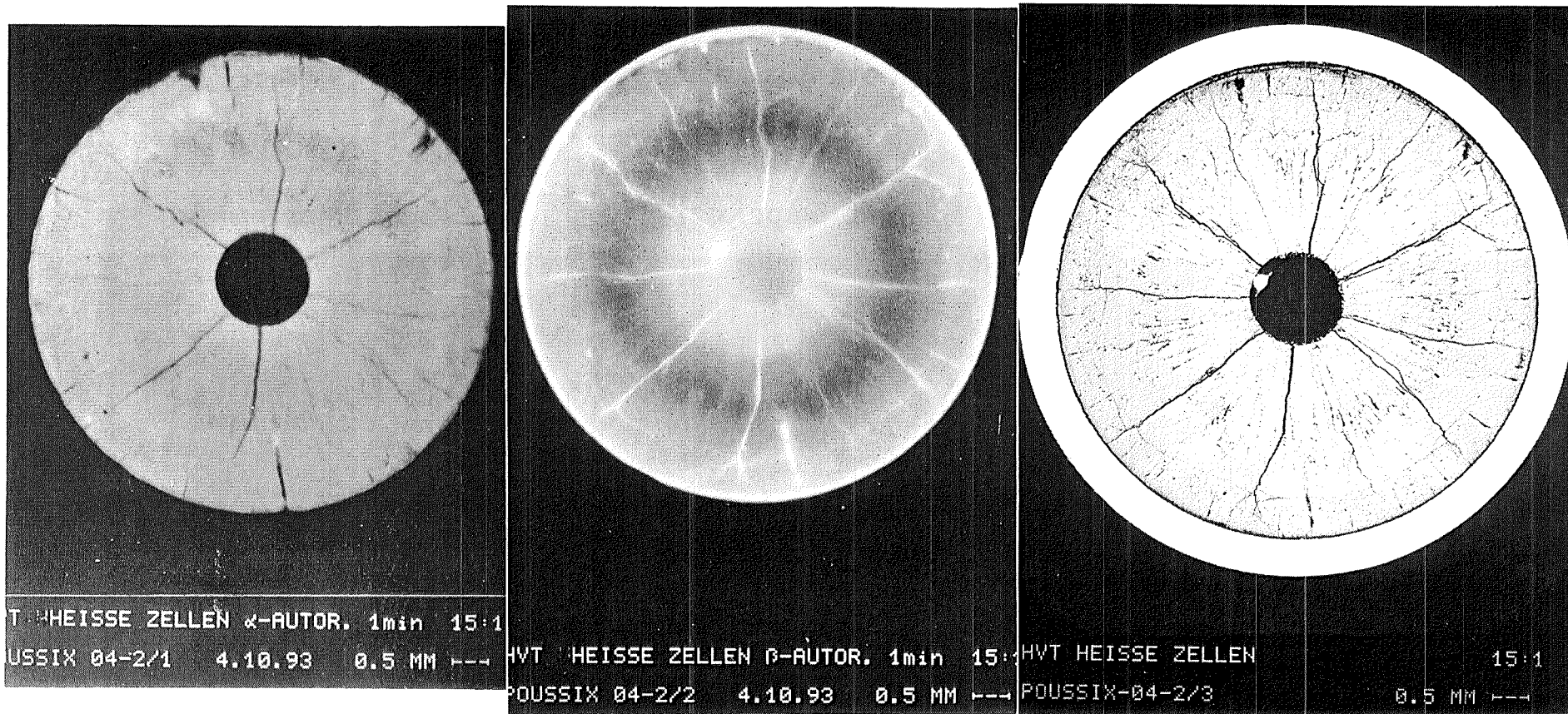
α-autoradiography   β-autoradiography   micrography

Fig. 15: Cross section at position 430 mm from lower fuel end of small gap pin 5/4 (T2)
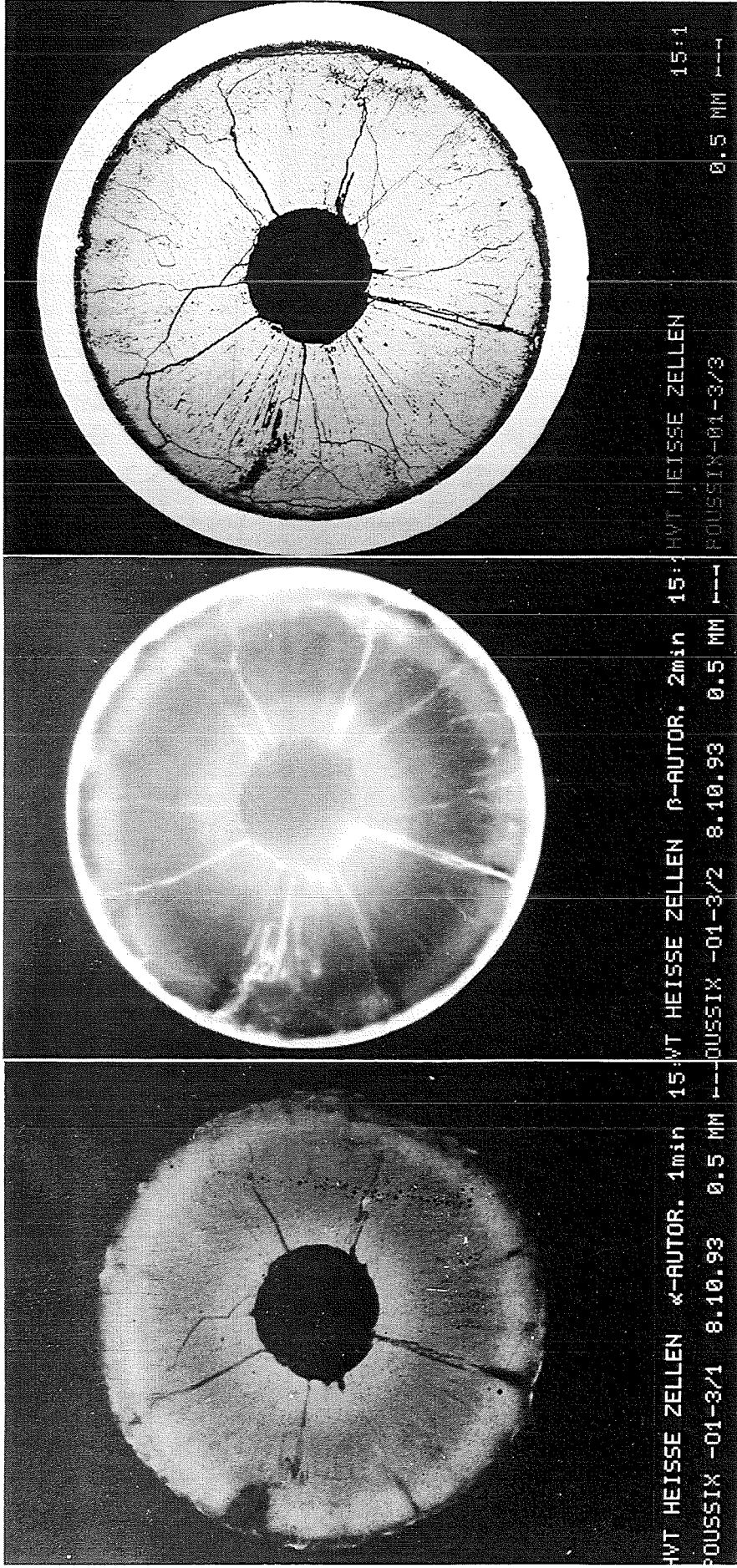
α-autoradiography β-autoradiography micrography

Fig. 16: Cross section at positon 430 mm from lower fuel end of annular pin 7/1 (T3)
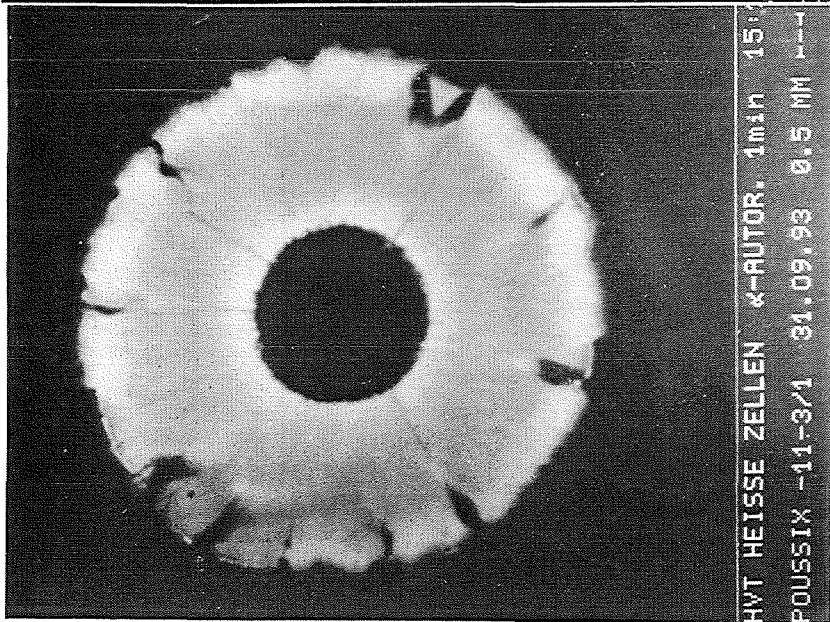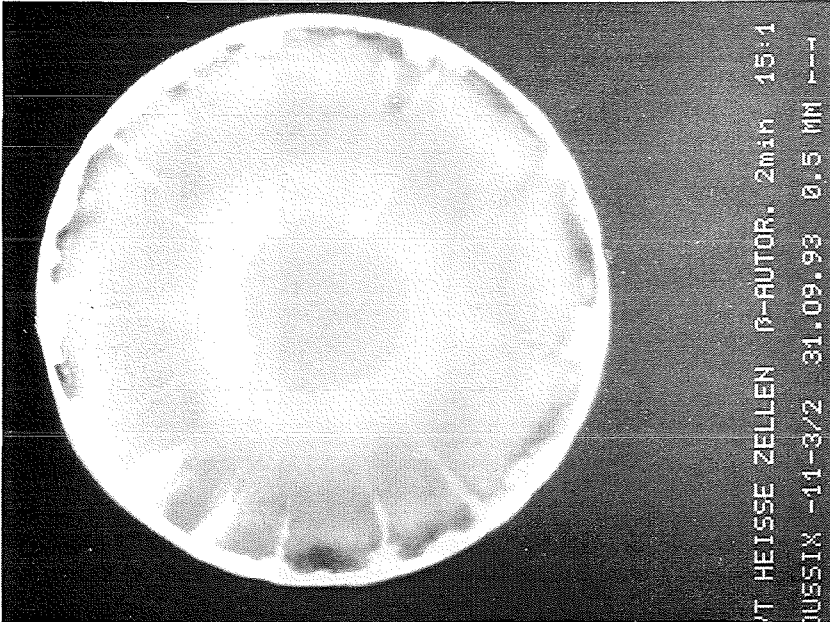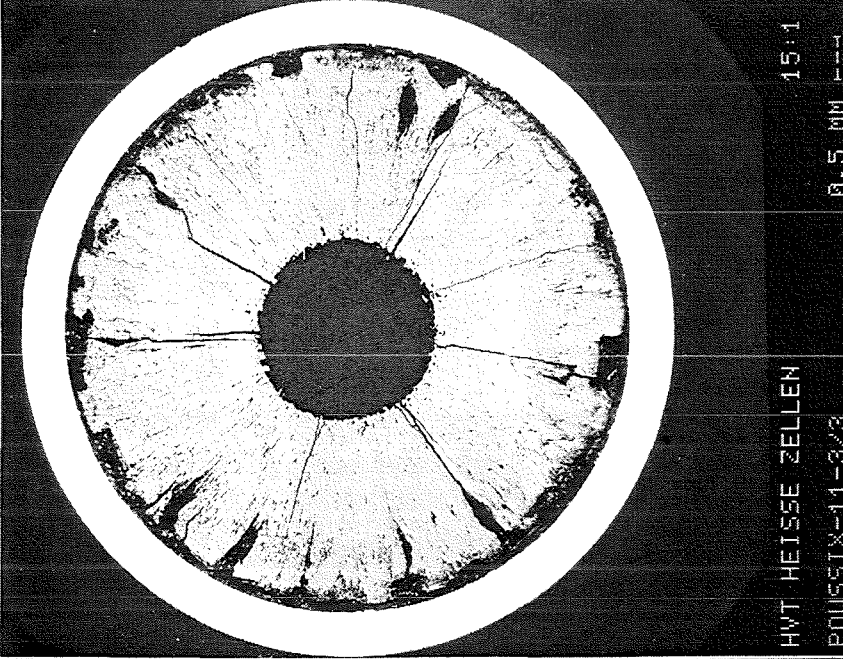
α-autoradiography β-autoradiography micrography

Fig. 17: Cross section at position 430 mm from lower fuel end of large gap pin 2/11 (T3)
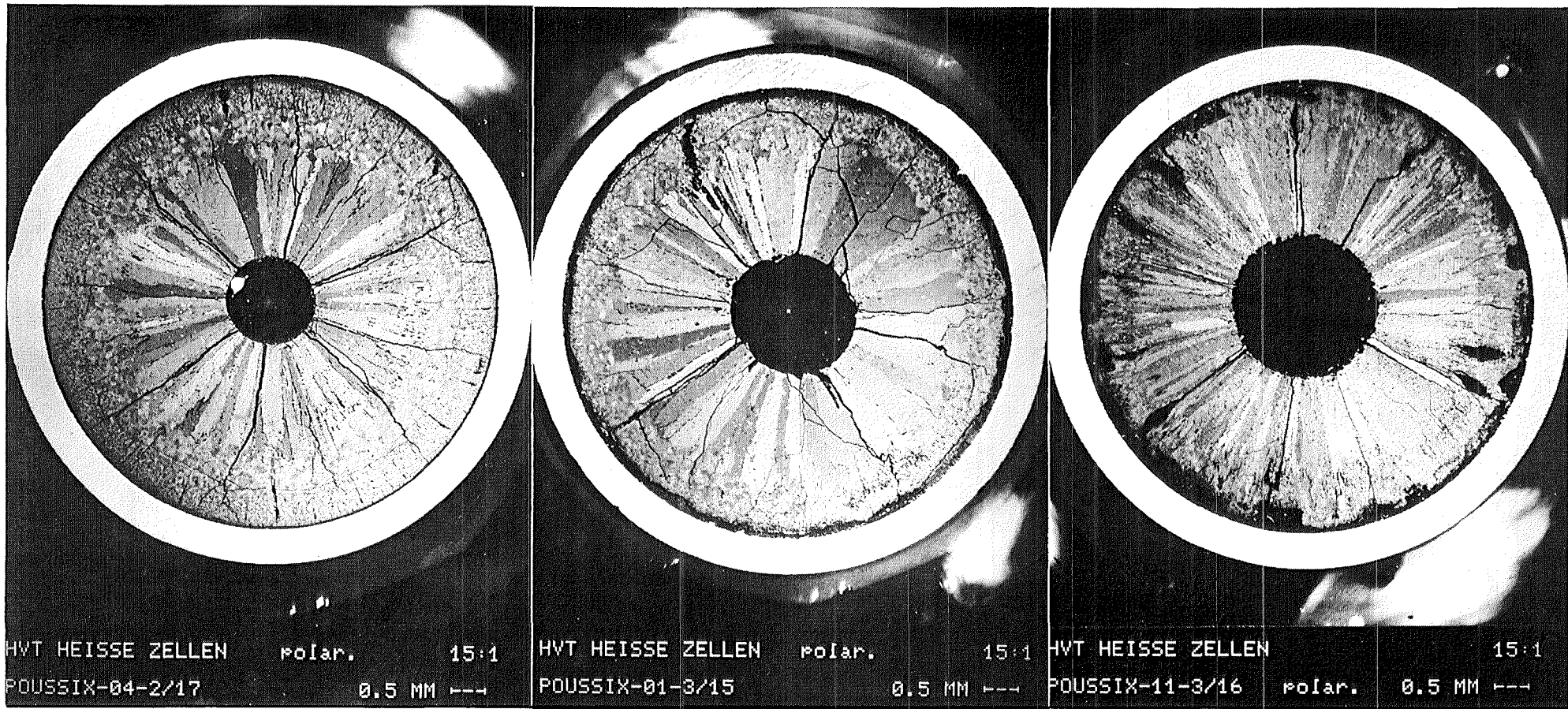
small gap pin 5/4

initial diam. gap: 127 μm

annular pin 7/1

initial diam.gap: 182 μm

large gap pin 2/11

initial diam. gap: 277 μm

Fig. 18: Polarized images of cross sections at positon 430 mm from lower fuel end of pins 5/4; 7/1 and 2/11
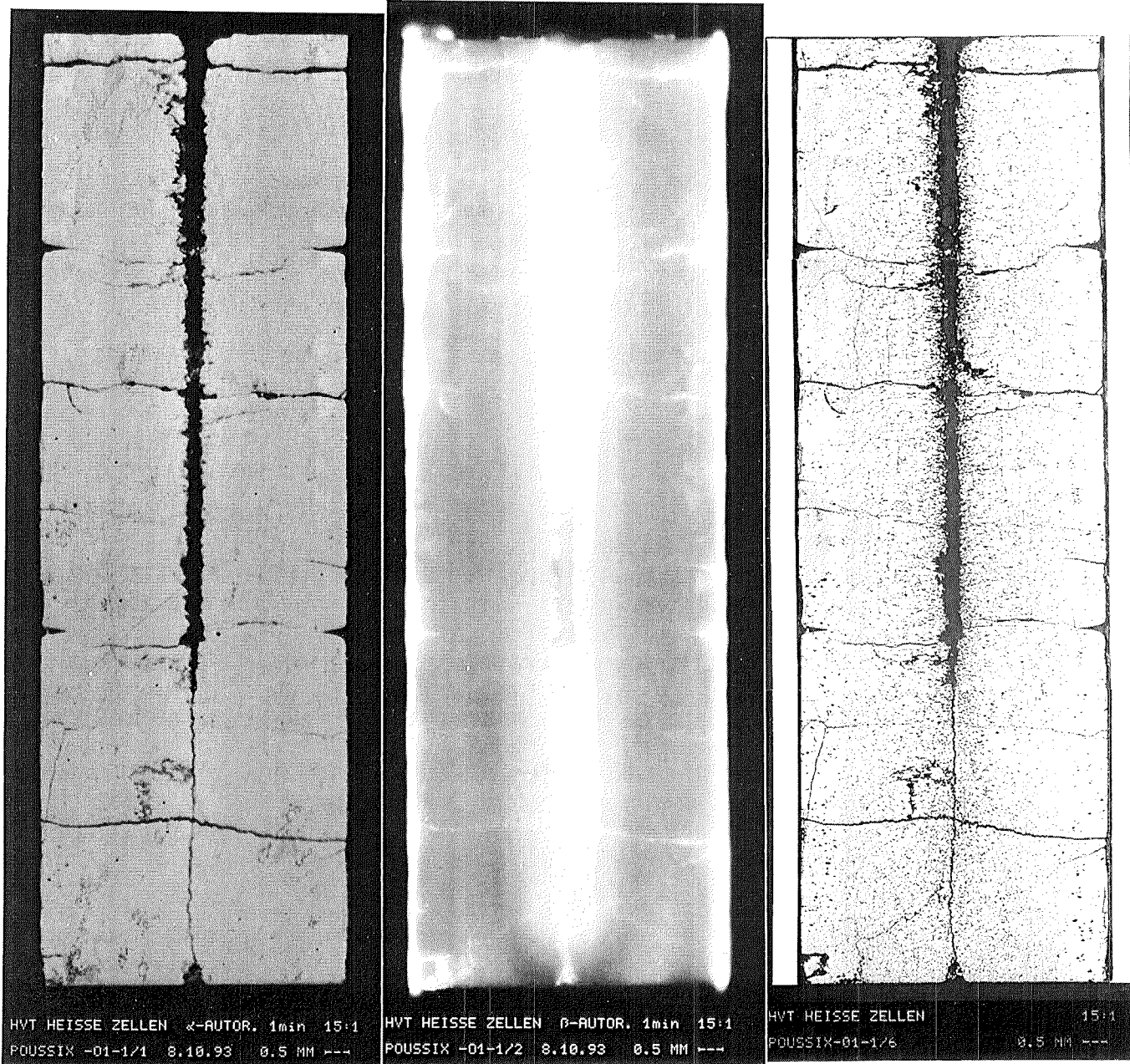
α-autoradiography   β-autoradiography   micrography

Fig. 19: Longitudinal cut at lower fuel/fertile interface of annular pellet pin 7/1 (L1)
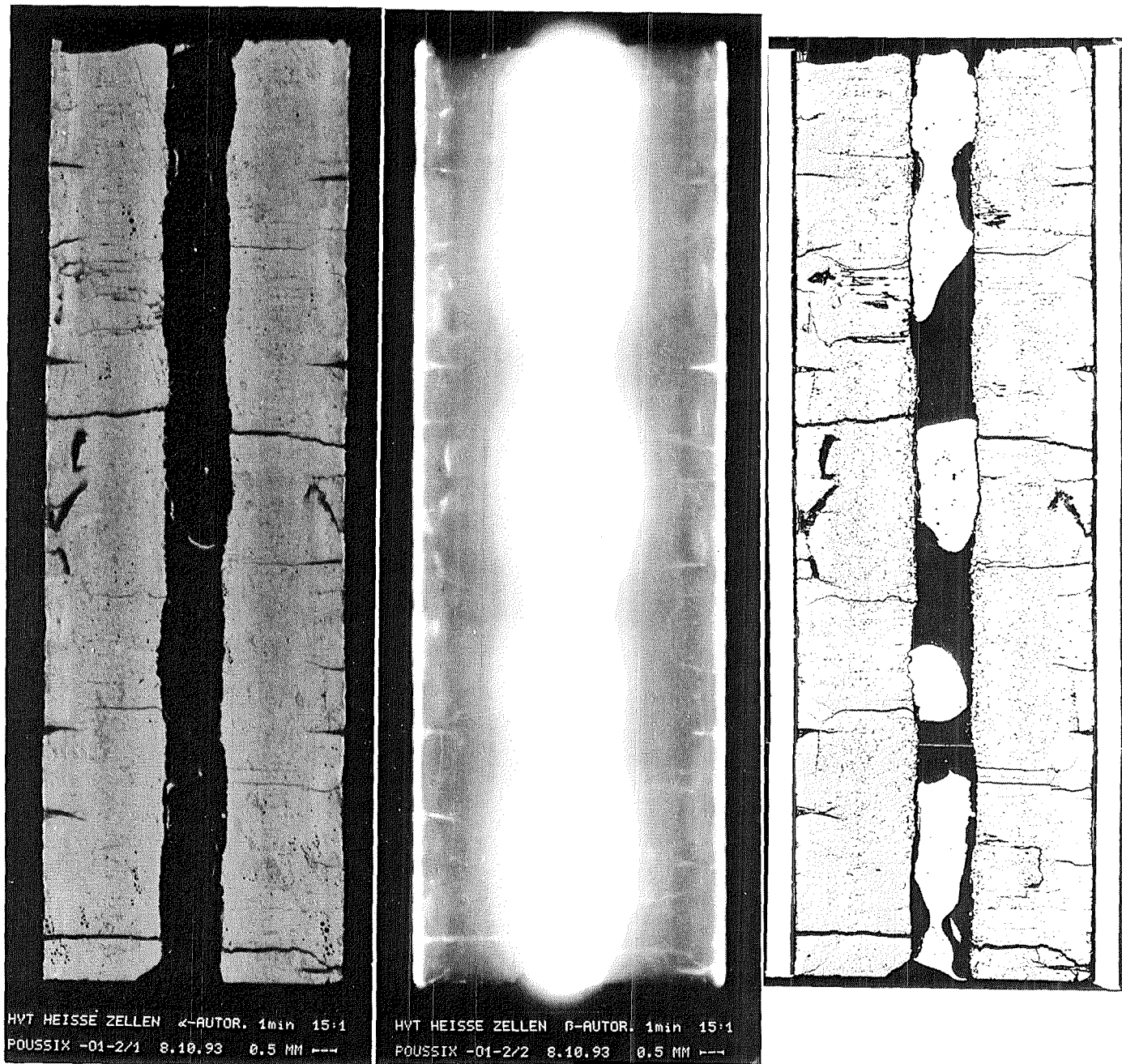
α-autoradiography   β-autoradiography   micrography

Fig. 20: Longitudinal cut about 120 mm above lower fuel end of annular pellet pin 7/1 (L2)
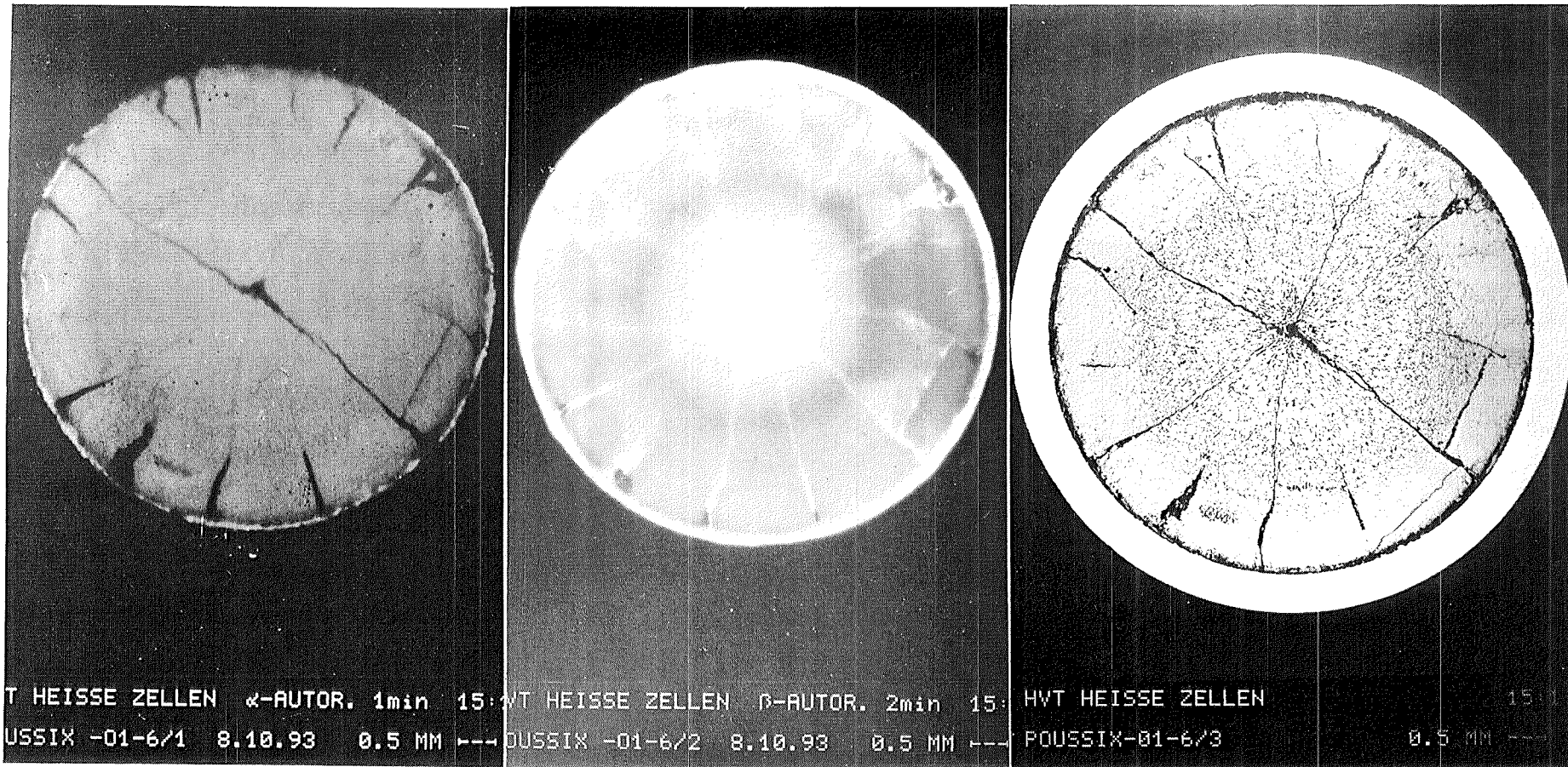
α-autoradiography   β-autoradiography   micrography

Fig. 21: Cross section about 65 mm below initial upper fuel/fertile interface of annular pellet pin 7/1 (T6)

| α-autoradiography | β-autoradiography | micrography |
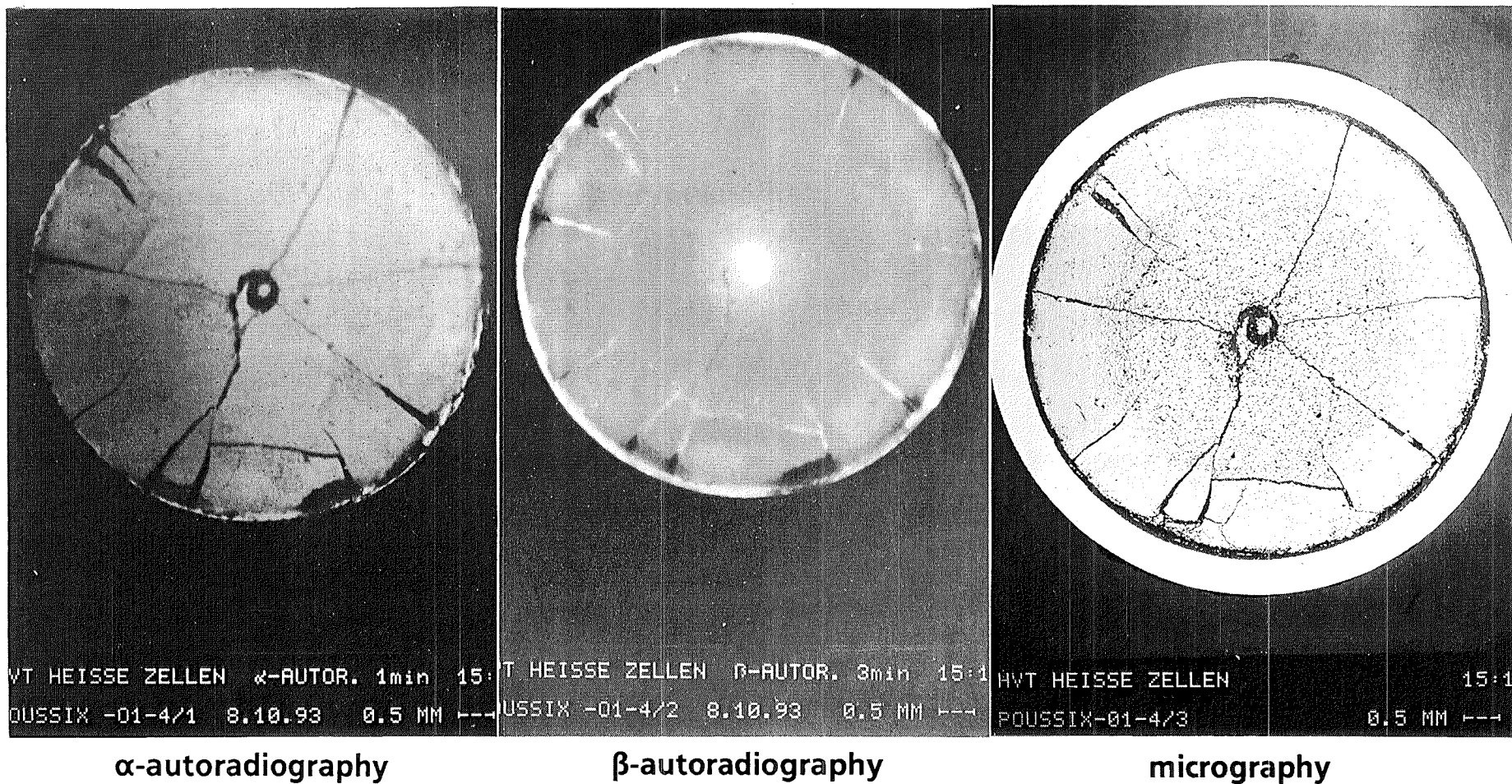
Fig. 22: Cross section about 25 mm below initial upper fuel/fertile interface of annular pellet pin 7/1 (T4)
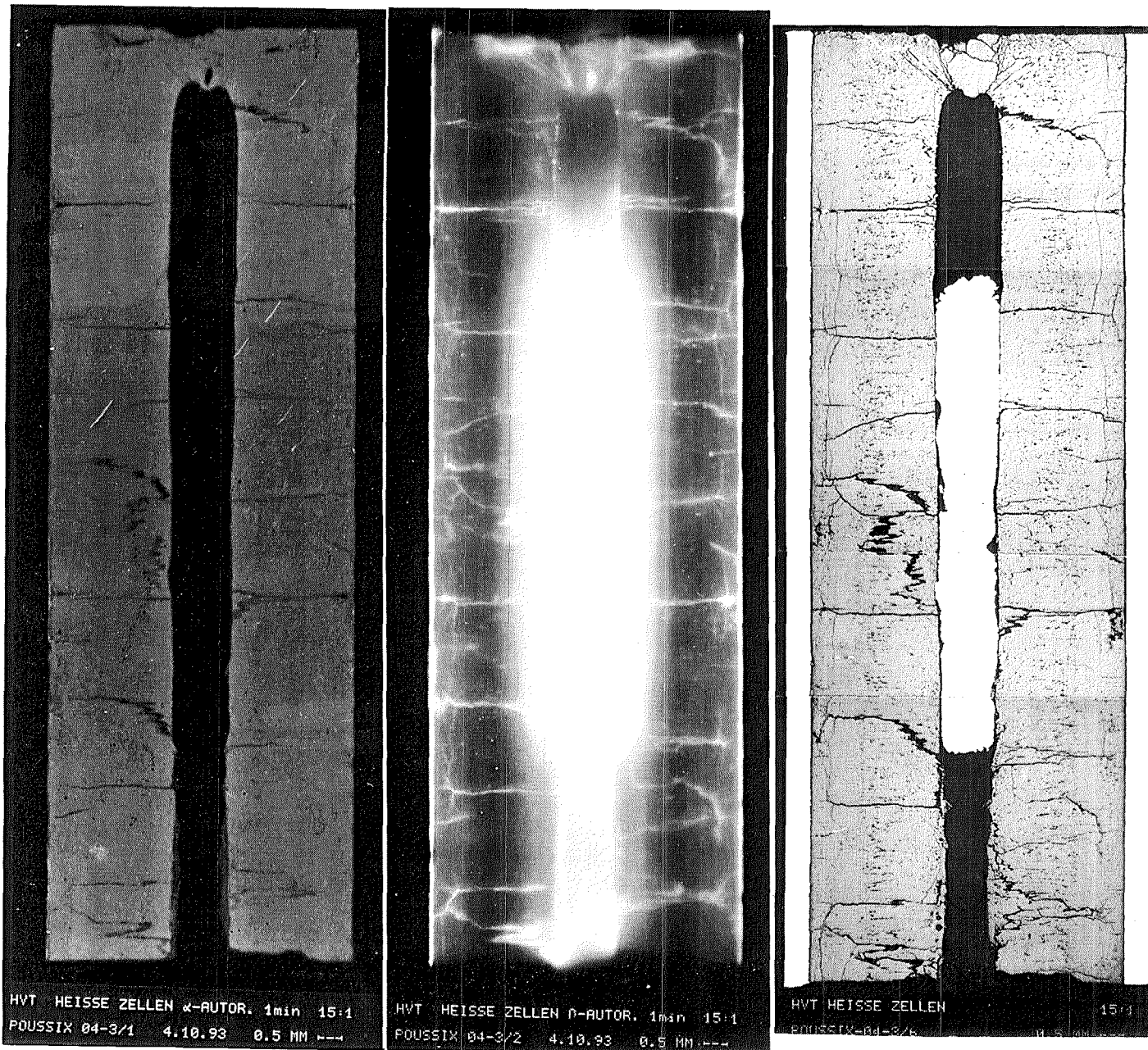
α-autoradiography   β-autoradiography   micrography

Fig. 23: Longitudinal cut about 70 mm above core centre line of small gap pin 5/4 (L3)
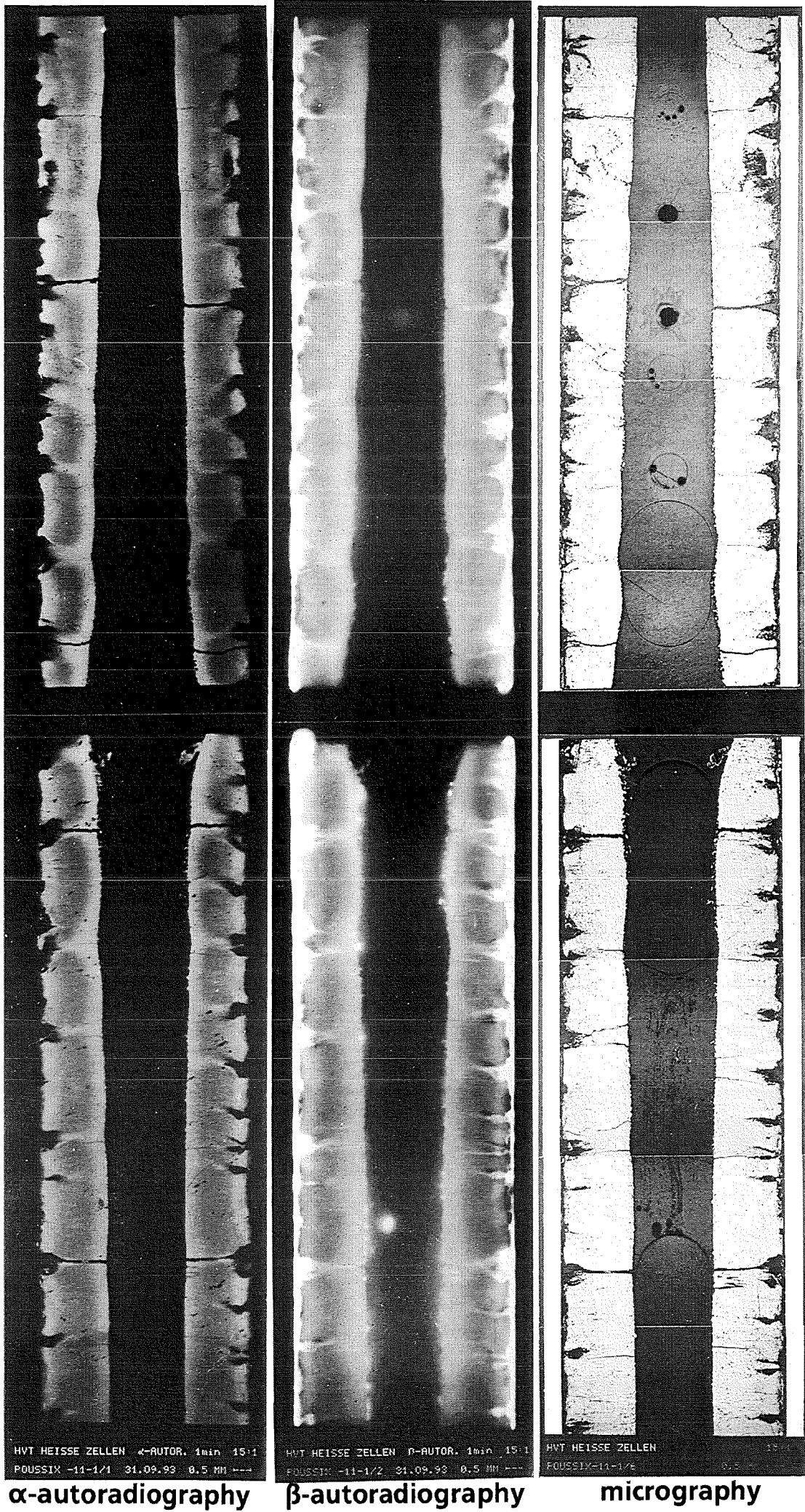
α-autoradiography   β-autoradiography   micrography

Fig. 24: Longitudinal cuts streching over the central channel opening of large gap pin 2/11 (L1 + L2)
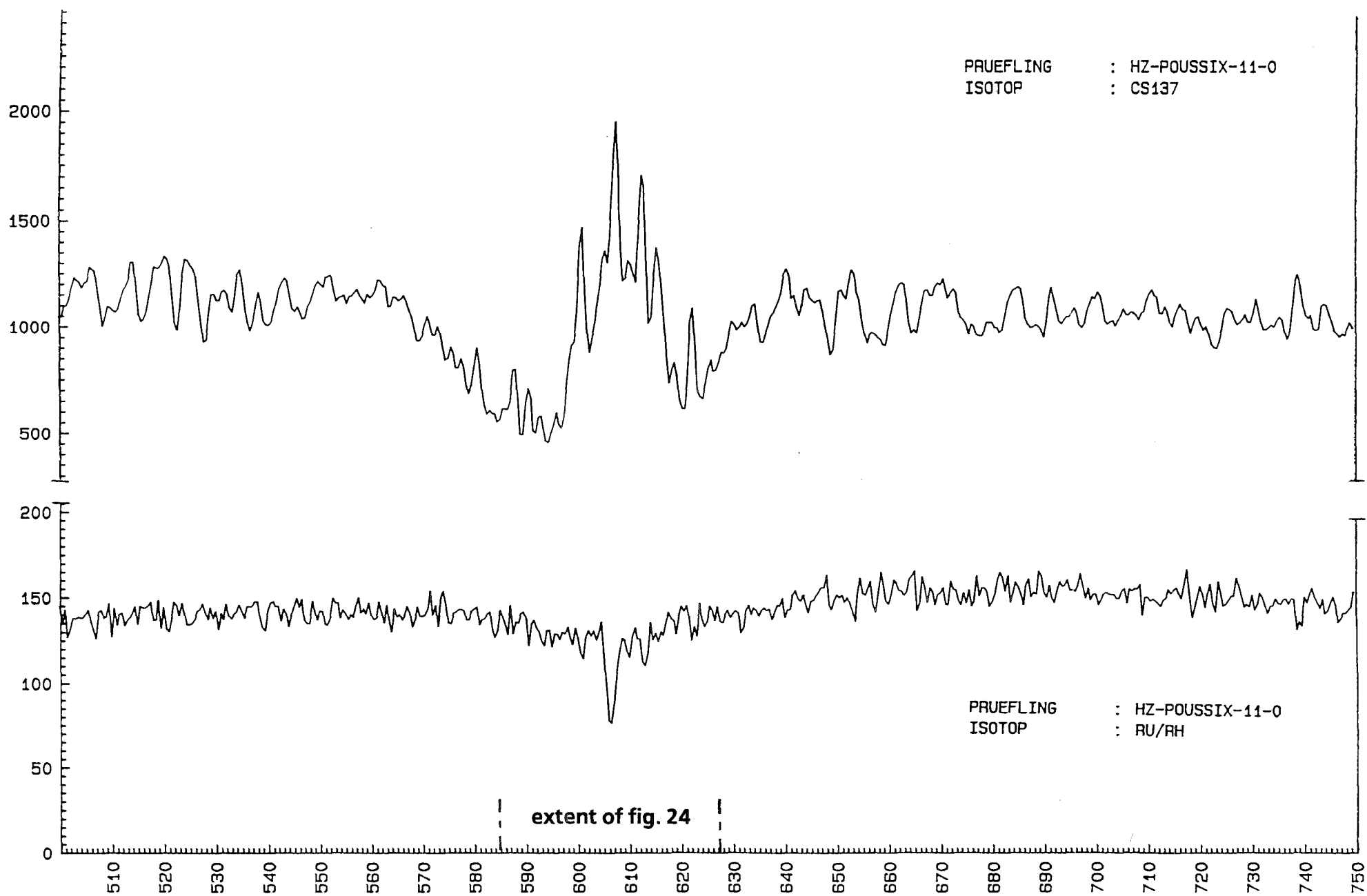
Fig. 25: Axial γ-scans for Cs-137 (upper trace) and Ru-106 (lower trace) over the region of central channel widening in large gap pin 2/11 (close-up on figs.10 and 14)
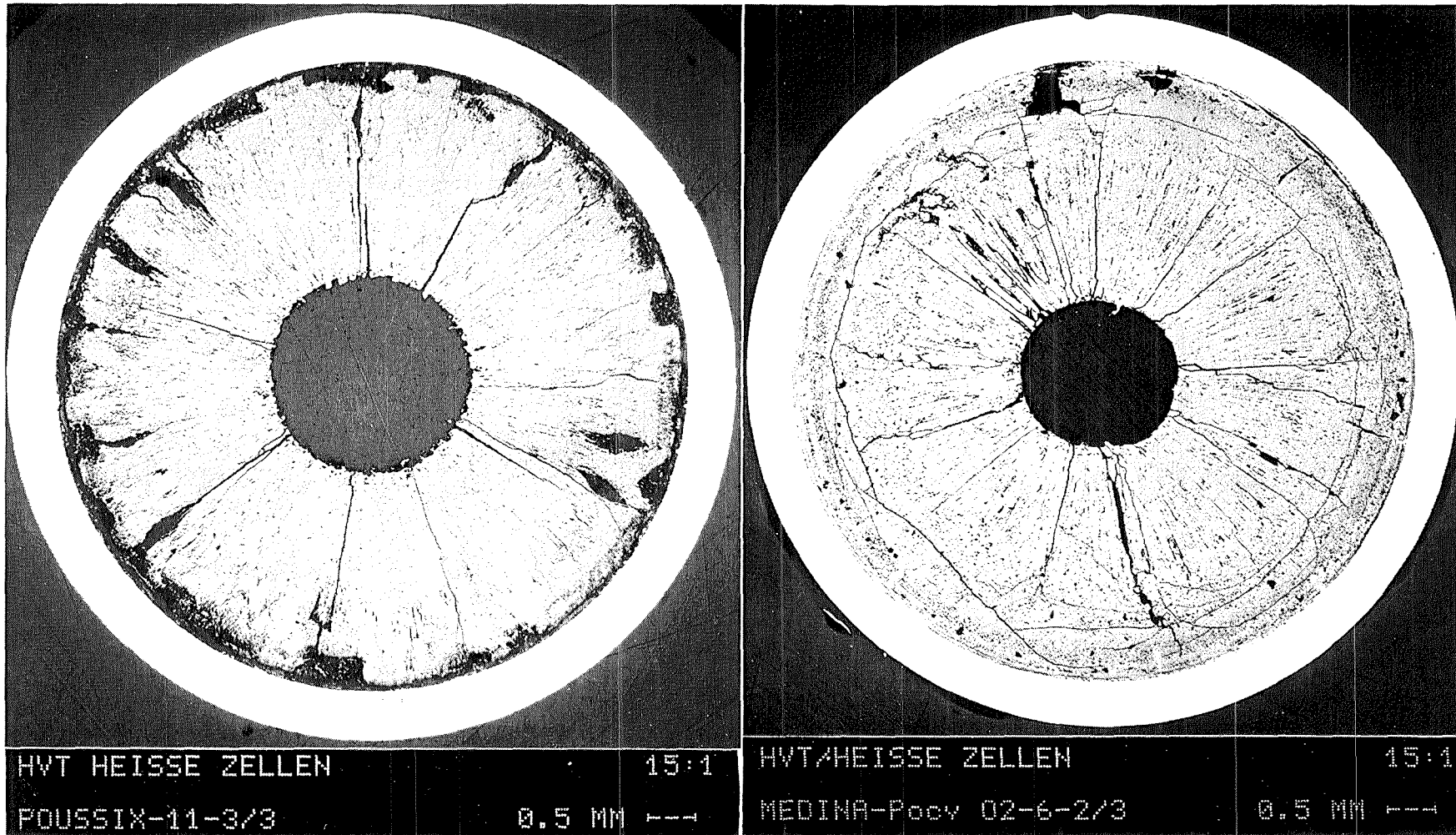
Fig. 26: Cross sections of fuel with an initial diametral gap of 275 µm

left: POUSSIX, fast flux, steady state operation;
max. linear rating: 415 W/cm; axial fuel
expansion; diametral increase due
to clad swelling: 25 µm

right: MEDINA, thermal flux, cyclic operation:
max. linear rating: 495 W/cm; no axial fuel
expansion; diametral increase due to FCMI: 15 µm
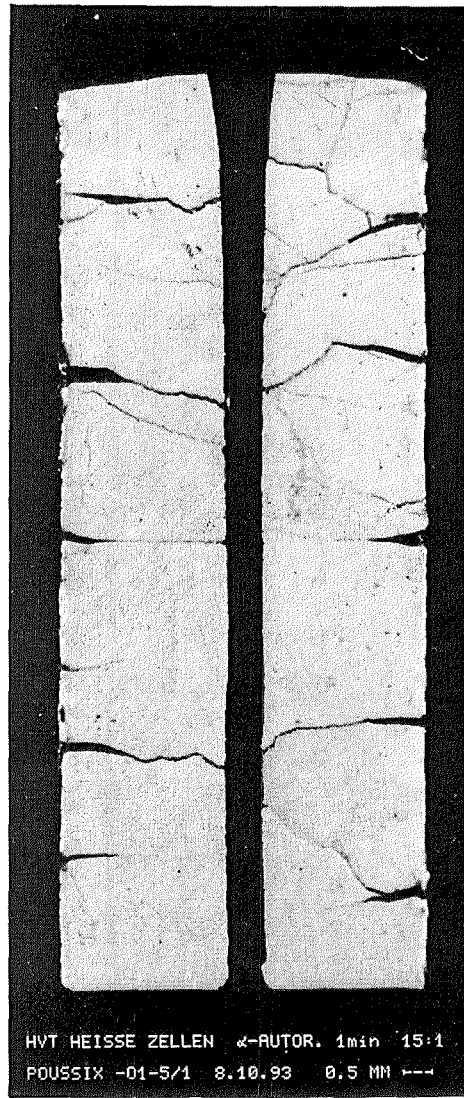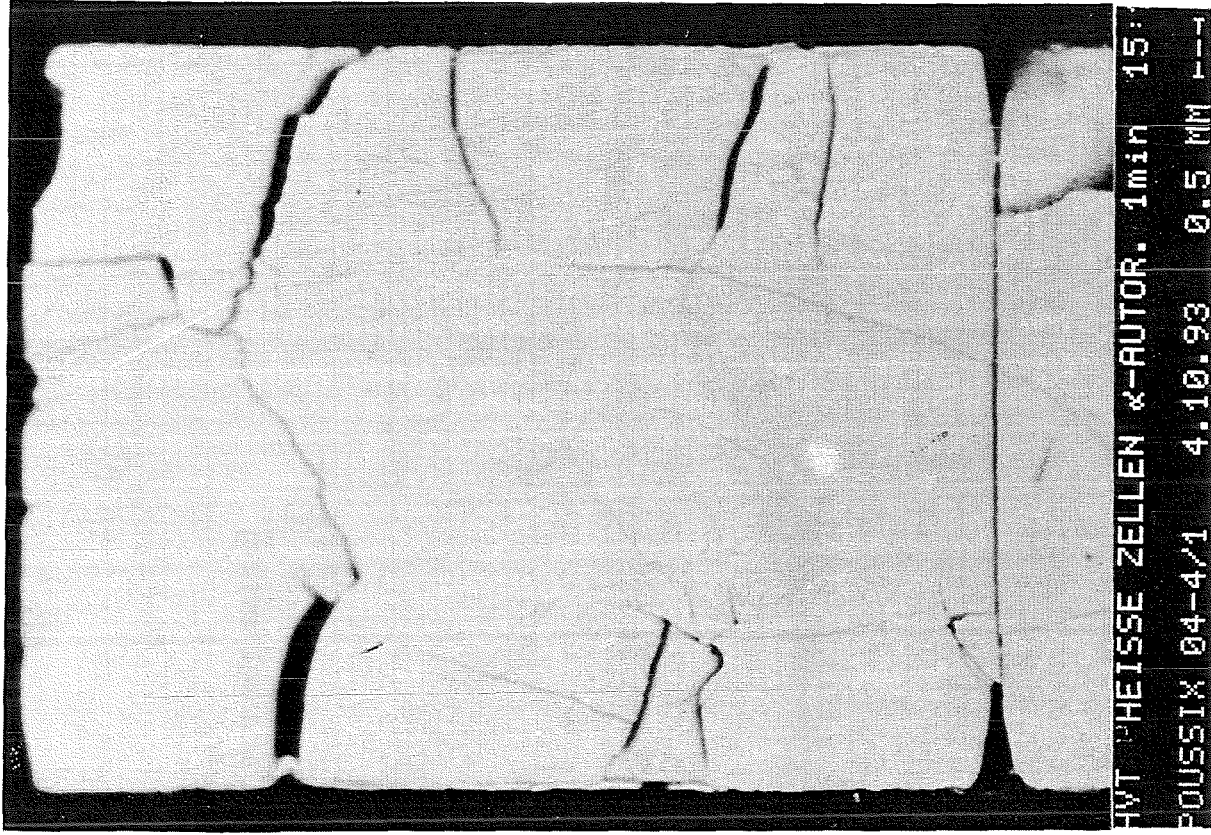
α-autoradiography
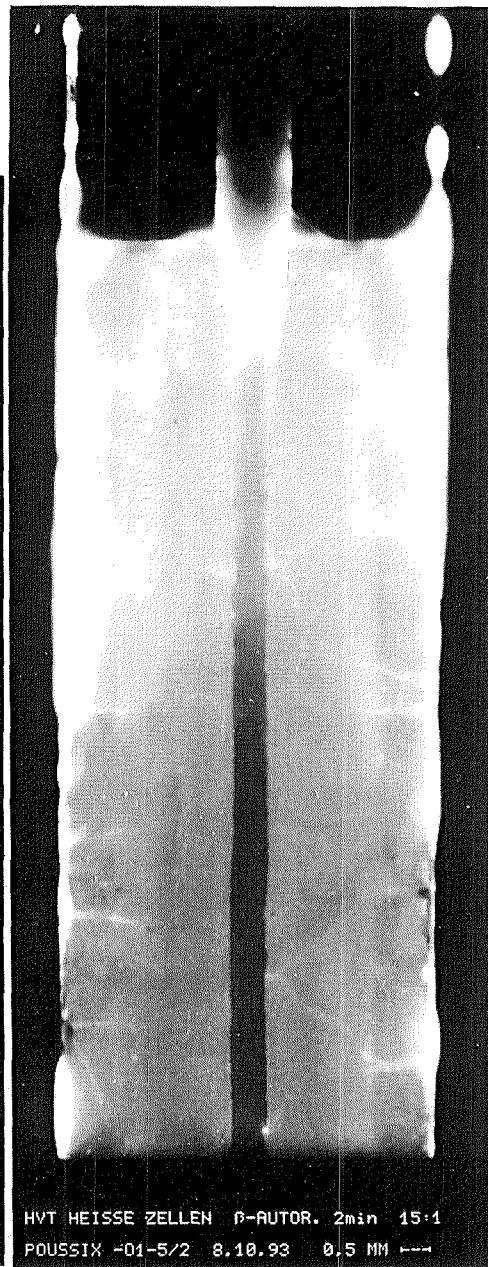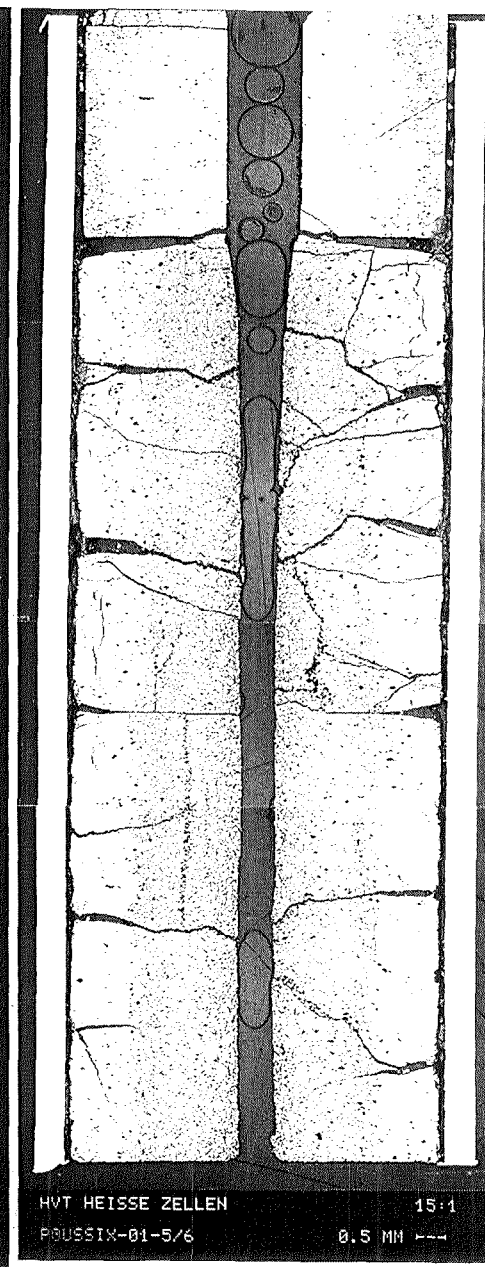
β-autoradiography

micrography

Fig. 27: Longidutinal cut at upper fuel/fertile interface of annular pellet pin 7/1 (L5)
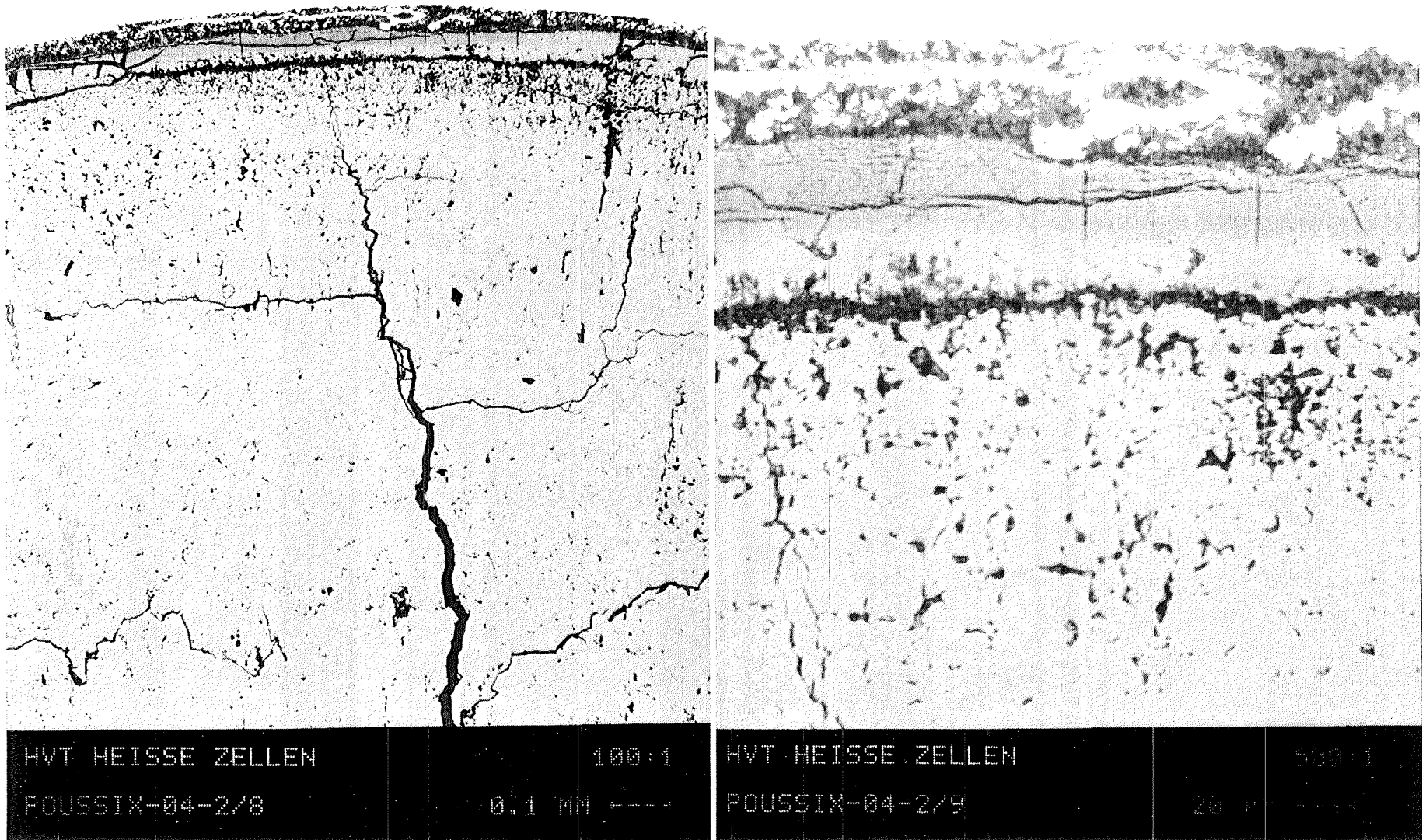
Fig. 28: Fuel layer on surface of pellet; detail from fig. 15. (T2 of pin 5/4)

α-autoradiography
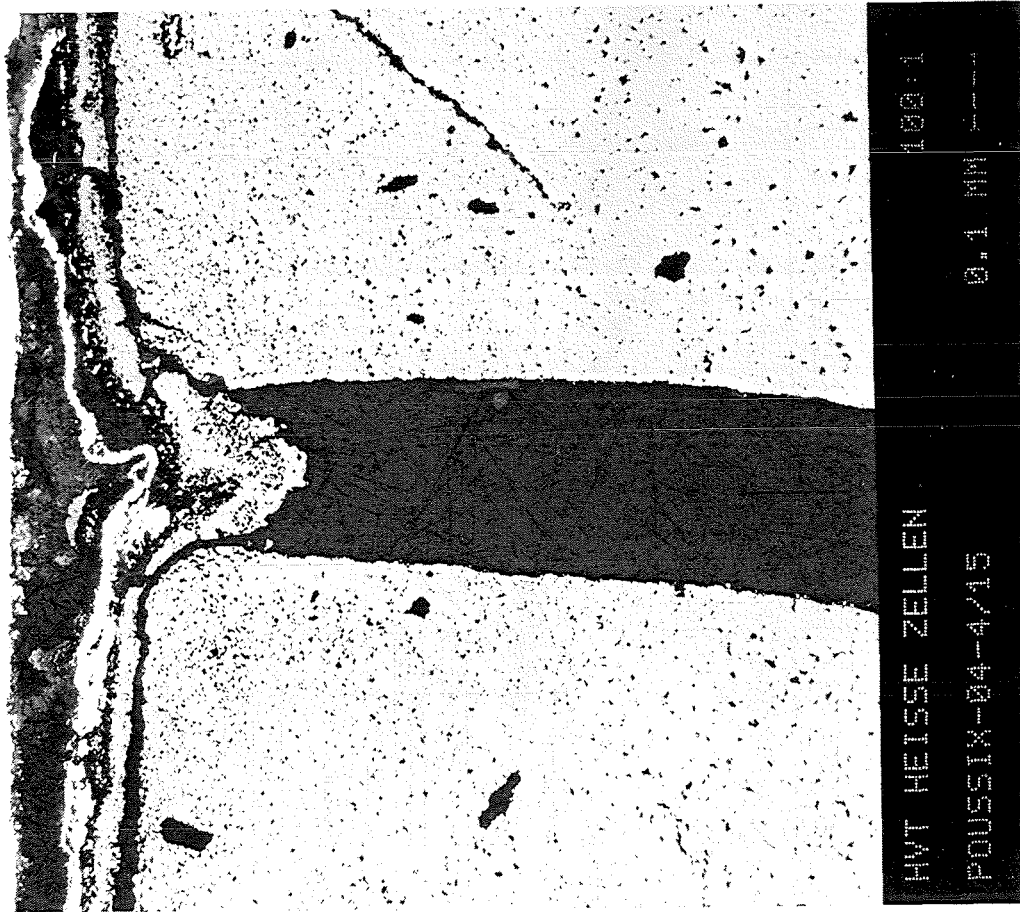
Fig. 29: Fuel layer on surface of pellet; detail from L4 of pin 5/4

EXPERIMENT   :   POUSSIX D183-60
PEN NUMBER   :   POU14/6
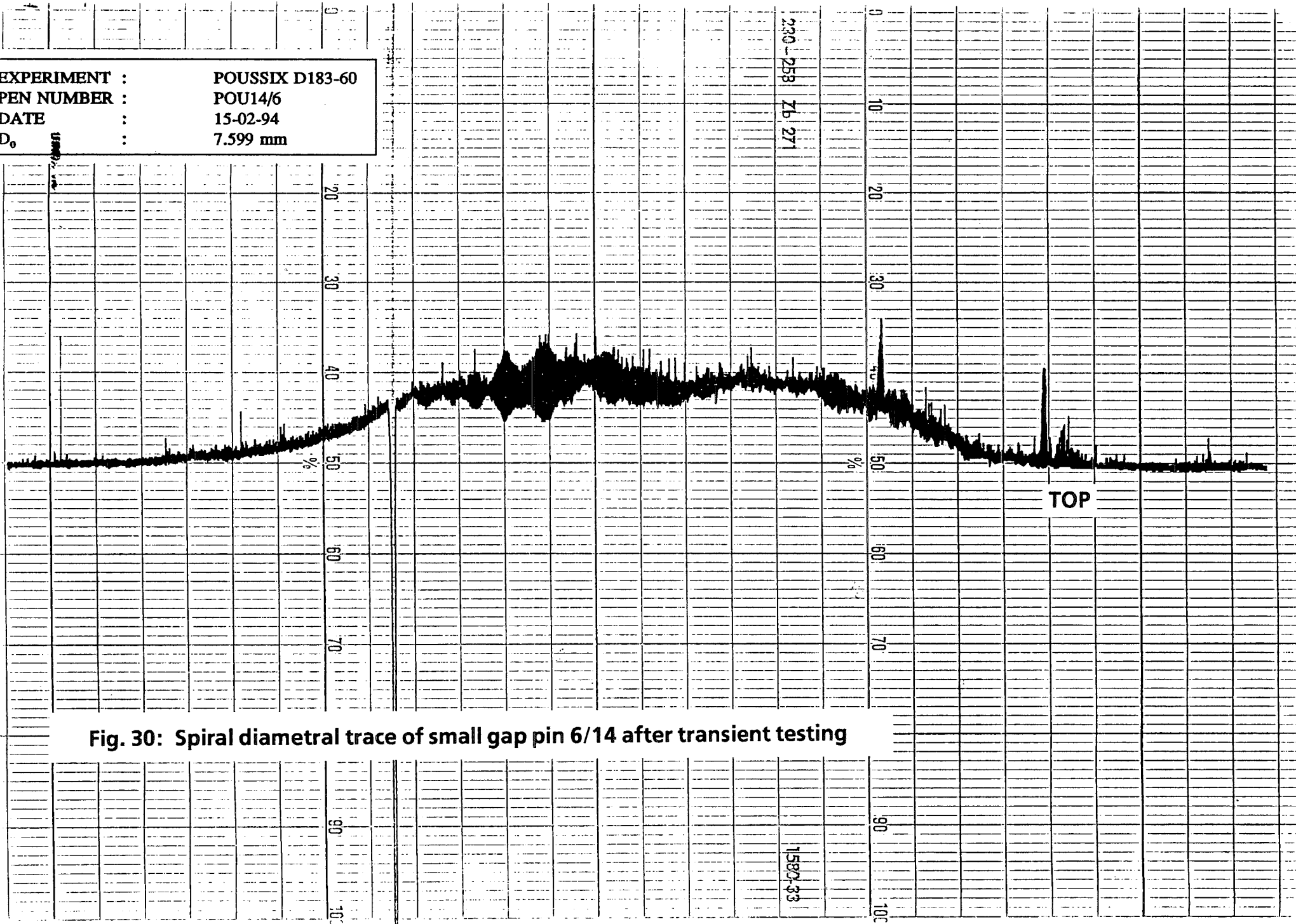DATE   :   15-02-94
D_0 :   7.599 mm

TOP

Fig. 30: Spiral diametral trace of small gap pin 6/14 after transient testing

EXPERIMENT	:	POUSSIX D183-59
PEN NUMBER	:	POU02/8
DATE	:	11-02-94
D_0	:	7.598 mm

TOP

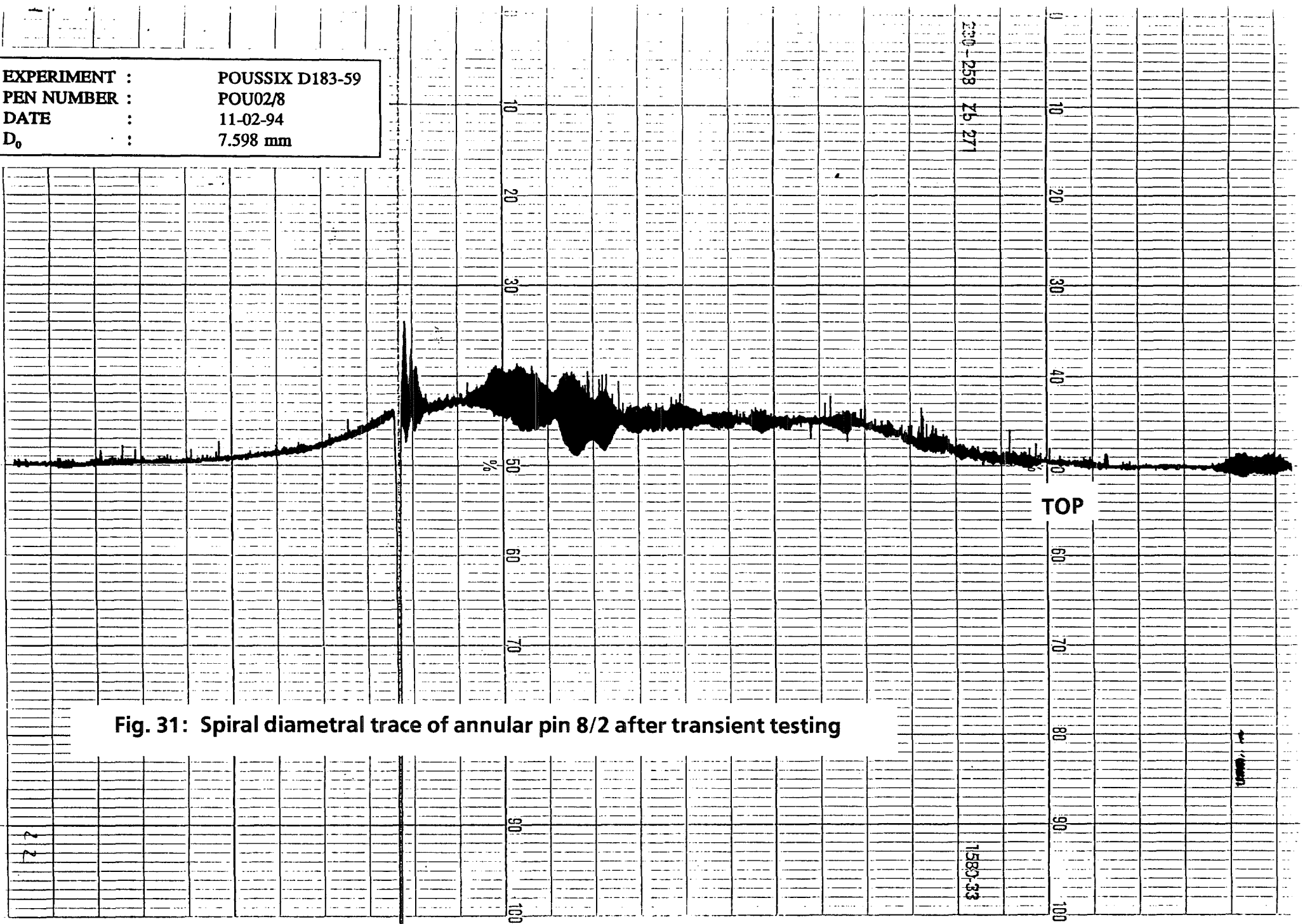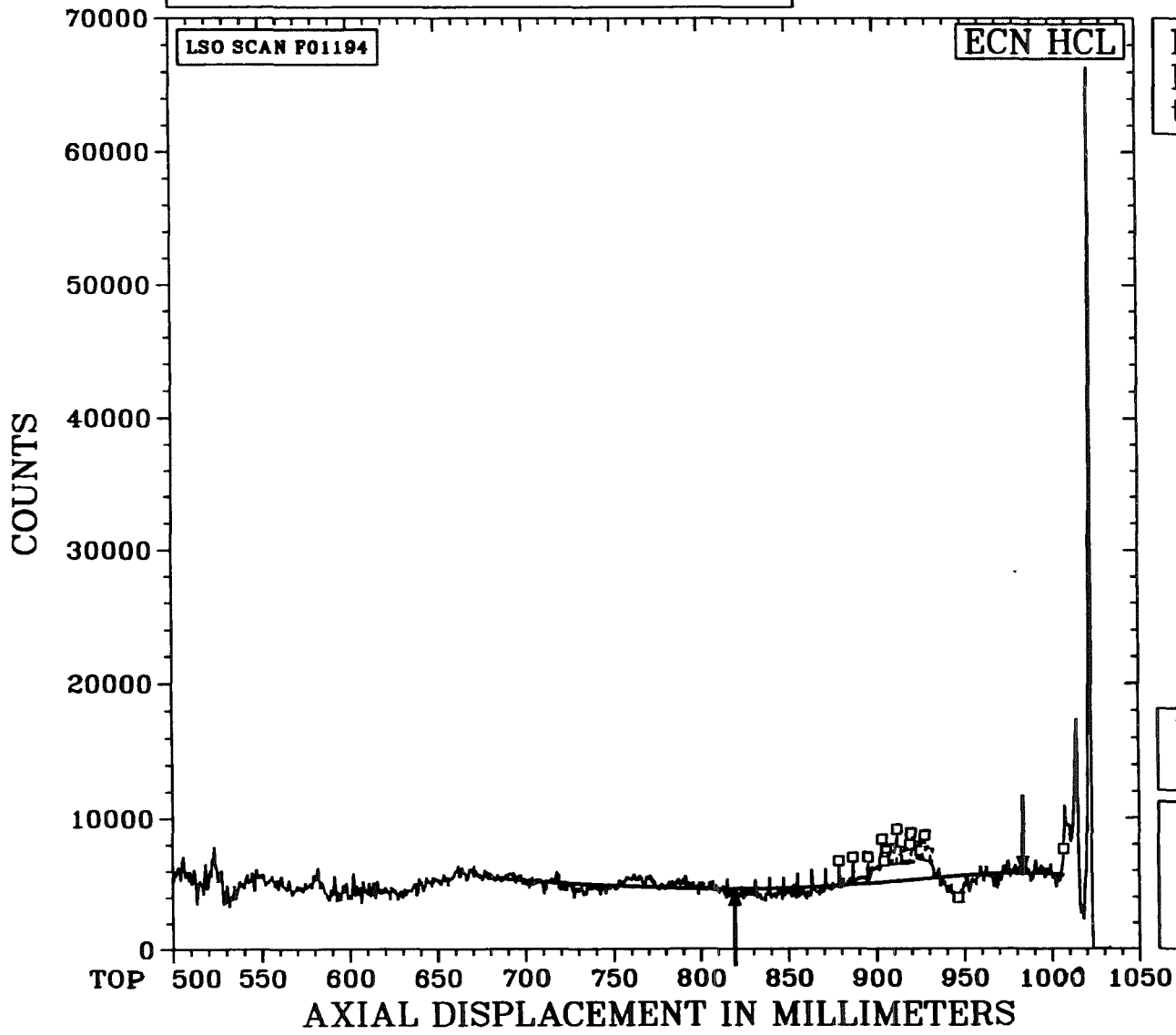**Fig. 31: Spiral diametral trace of annular pin 8/2 after transient testing**

EXPERIMENT : D183−59 POU02/8
DATE : 10−12−93

LSO SCAN F01194

ECN HCL

Nuclide : CS−137
Energy : 661.66 keV
$t_{1/2}$: 30.00 years

Fig. 32: Axial γ-scan for Cs-137

of annular pin 8/2 after

power transient in HFR

Decay correction :
from 09−12−93 22:40:10

——— : counts
——— : least−squares curve
□ : peak or dip
——→ : maximum, minimum

COUNTS

70000
60000
50000
40000
30000
20000
10000
0

TOP 500 550 600 650 700 750 800 850 900 950 1000 1050

AXIAL DISPLACEMENT IN MILLIMETERS

LSO SCAN F01197

ECN HCL

Nuclide : CS−137
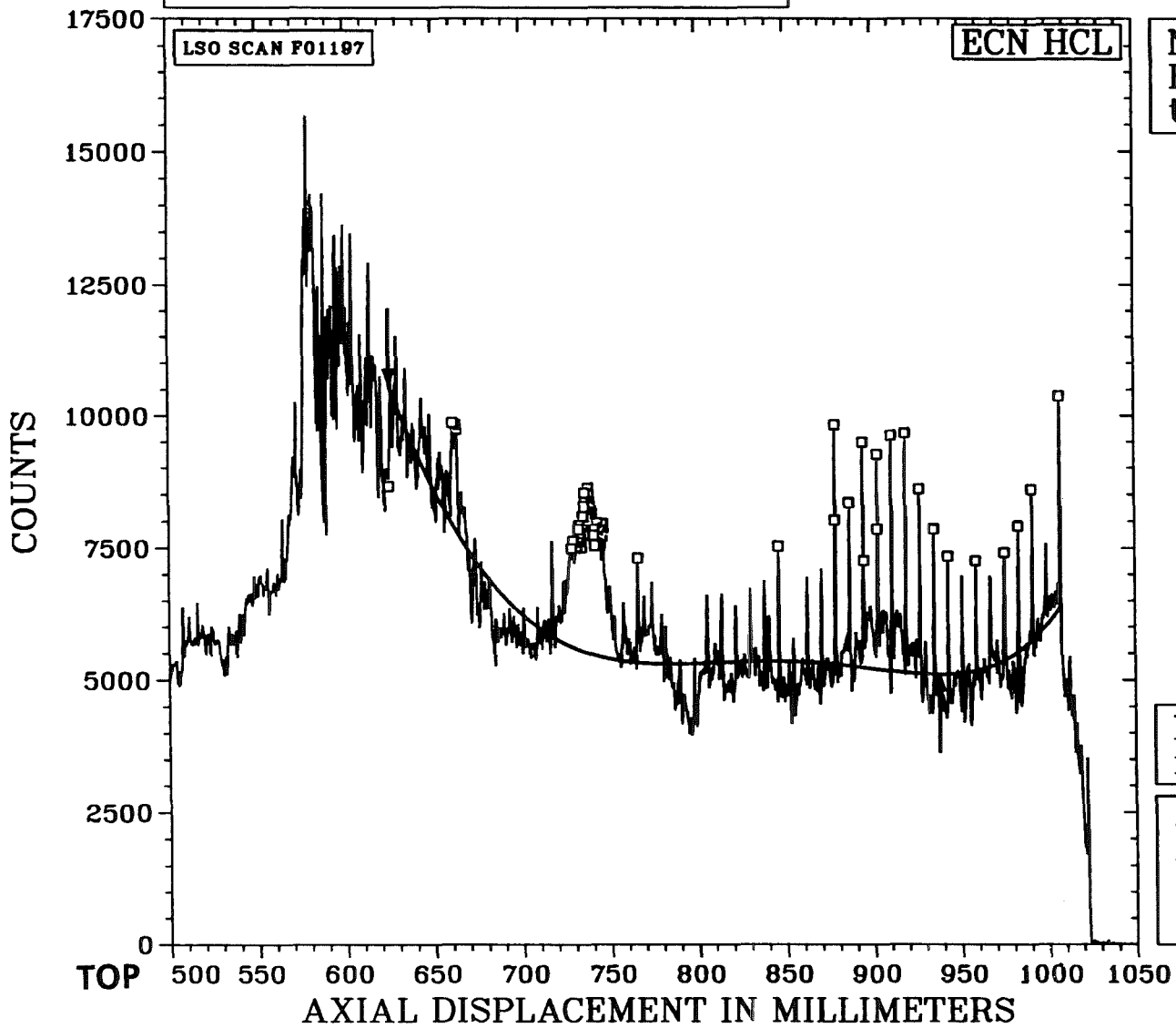Energy : 661.66   keV
$t_{1/2}$: 30.00 years

Fig. 33: Axial γ-scan for Cs-137

of small gap pin 6/14 after

power transient in HFR

Decay correction :
from   09−12−93 22:40:10

――― : counts
――― : least−squares curve
 □   : peak or dip
――→ : maximum, minimum

17500

15000

12500

10000

7500

5000

2500

0

COUNTS

TOP   500 550   600   650   700   750   800   850   900   950   1000 1050

AXIAL DISPLACEMENT IN MILLIMETERS